Annual Review of Marine Science

The Origin of Modern Atolls: Challenging Darwin's Deeply Ingrained Theory

André W. Droxler[1] and Stéphan J. Jorry[2]

[1]Department of Earth, Environmental, and Planetary Sciences, Rice University, Houston, Texas 77005, USA; email: andre@rice.edu

[2]Marine Geosciences Unit, IFREMER, 29280 Plouzané, France

Annu. Rev. Mar. Sci. 2021. 13:21.1–21.37

The *Annual Review of Marine Science* is online at marine.annualreviews.org

https://doi.org/10.1146/annurev-marine-122414-034137

Keywords

atoll origin, flat-topped bank, sea level, karstification, Plio-Pleistocene, Indian Ocean, Pacific Ocean, Maldives

Abstract

In 1842, Darwin identified three types of reefs: fringing reefs, which are directly attached to volcanic islands; barrier reefs, which are separated from volcanic islands by lagoons; and ring reefs, which enclose only a lagoon and are defined as atolls. Moreover, he linked these reef types through an evolutionary model in which an atoll is the logical end point of a subsiding volcanic edifice, as he was unaware of Quaternary glaciations. As an alternative, starting in the 1930s, several authors proposed the antecedent karst model; in this model, atolls formed as a direct interaction between subsidence and karst dissolution that occurred preferentially in the bank interiors rather than on their margins through exposure during glacial lowstands of sea level. Atolls then developed during deglacial reflooding of the glacial karstic morphologies by preferential stacked coral-reef growth along their margins. Here, a comprehensive new model is proposed, based on the antecedent karst model and well-established sea-level fluctuations during the last 5 million years, by demonstrating that most modern atolls from the Maldives Archipelago and from the tropical Pacific and southwest Indian Oceans are rooted on top of late Pliocene flat-topped banks. The volcanic basement, therefore, has had no influence on the late Quaternary development of these flat-topped banks into modern atolls. During the multiple glacial sea-level lowstands that intensified throughout the Quaternary, the tops of these banks were karstified; then, during each of the five mid-to-late Brunhes deglaciations, coral reoccupied their raised margins and grew vertically, keeping up with sea-level rise and creating the modern atolls.

1. INTRODUCTION

In 1842, Darwin explained atolls as the ultimate evolution phase of initial fringing and subsequent barrier reefs attached to subsiding volcanic islands (Darwin 1842). During his five-year voyage around the world on the HMS *Beagle* (1831–1836), Darwin visited Chile for some time. The observation of vertical tectonic motion, located along a fault zone linked to a major Chilean earthquake, made him believe that the existence of continents was related to an overall uplift, whereas oceans were formed through the slow subsidence of the ocean floor, explaining their abyssal depths. Although Darwin sailed close to some Pacific atolls and spent some time in Tahiti (**Figure 1**), he studied only one true atoll on the *Beagle* expedition, when he stopped in the southeastern equatorial Indian Ocean at Cocos Atoll of the Keeling Islands (**Figure 1**). During the stop, he observed, mapped, and gathered samples from the islands and the surrounding coral reefs and lagoons. In addition to his direct observations of Cocos Atoll, Darwin had, during his voyage, access to multiple British nautical charts on which coral reefs—significant navigation hazards—had been mapped in great detail and with surprisingly high accuracy.

Based on these charts, Darwin compiled the first world map of coral reefs, which was included in his 1842 publication (Darwin 1842) and was similarly astonishing in its accuracy. On this map, he identified three types of reefs: fringing reefs, which are directly attached to volcanic islands; barrier reefs, which are separated from volcanic islands by lagoons; and ring reefs, which enclose only a lagoon, defined as an atoll. [The term atoll comes from the word *atholhu* in the Dhivehi language spoken on the Maldive Islands, meaning the palm of the hand; its first recorded use in English was as "atollon," in 1625 (Wikipedia 2020).] He linked those three types of reefs together

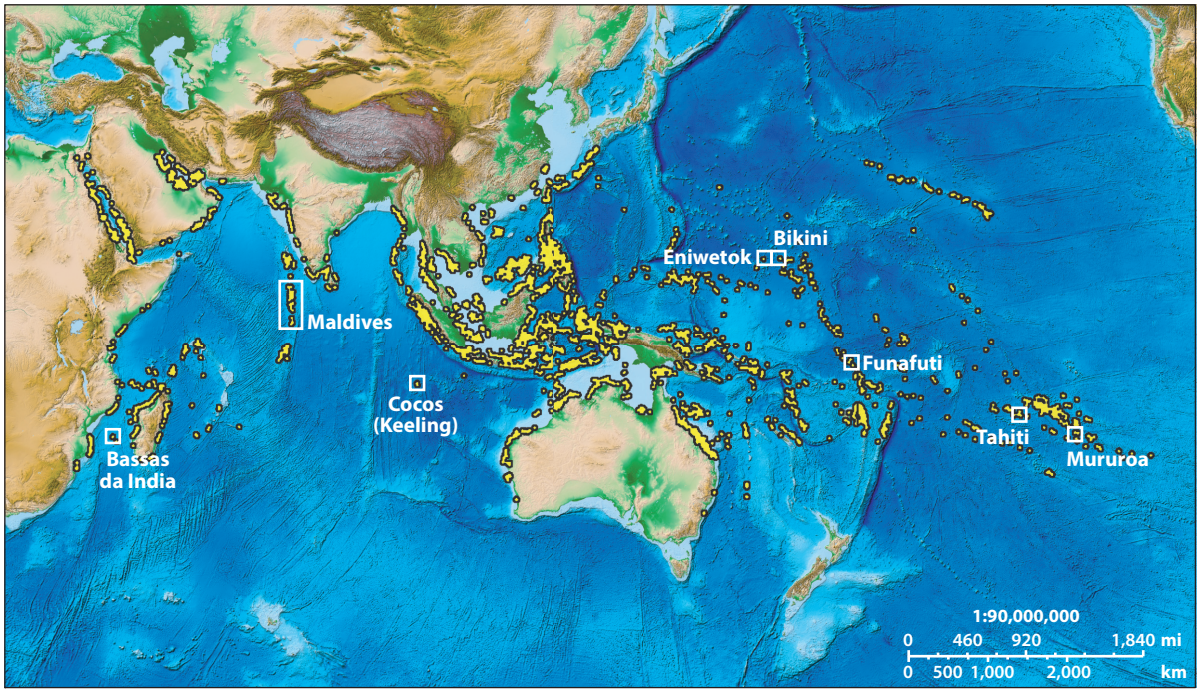

Figure 1

Locations of the atoll sites described in this review on the ETOPO1 Global Relief Model (Amante & Eakins 2009). Yellow areas illustrate the distribution of modern coral reefs (UNEP-WCMC et al. 2018).

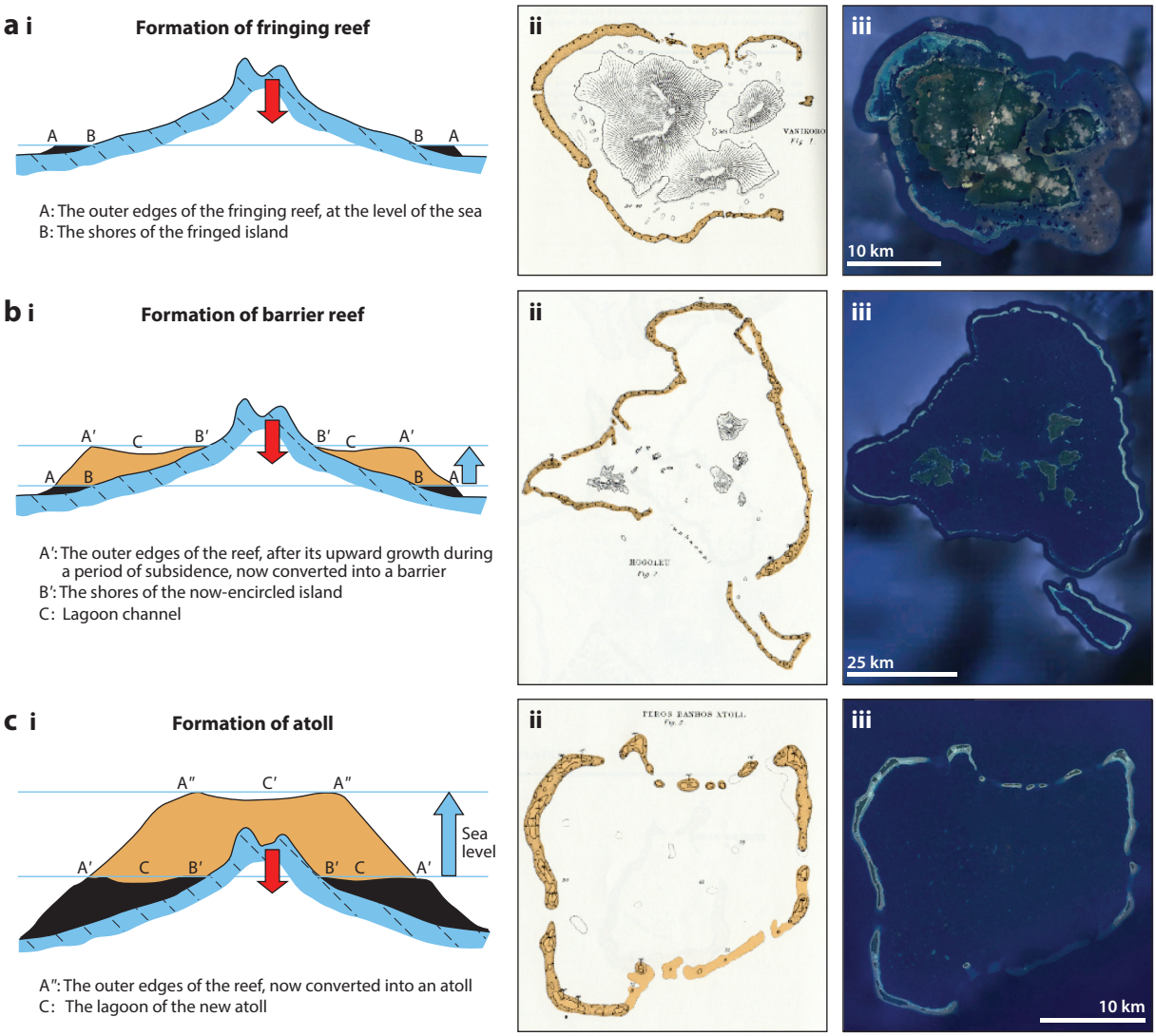

Figure 2

Darwin's subsidence model for the formation of (*a*) fringing reefs, (*b*) barrier reefs, and (*c*) atolls. The left subpanels show 2D models adapted from Darwin (1842). The center and right subpanels show maps from Darwin (1842) and the corresponding Google Earth satellite images, respectively, for the Vanikoro fringing reef, Solomon Islands (panel *a*, subpanels *ii* and *iii*); the Chuuck barrier reef, Micronesia (panel *b*, subpanels *ii* and *iii*); and Peros Banhos Atoll, Chagos Archipelago (panel *c*, subpanels *ii* and *iii*). Subpanels *i* and *ii* in all panels adapted from Darwin (1842).

in an evolutionary model that elegantly explained their interrelated origin through the slow and steady subsidence of the volcanic edifices (**Figure 2**). He initially presented his atoll observations and his model of how they formed in a well-received lecture given at the Geological Society of London on May 31, 1837, and his subsequent 1842 publication was illustrated with multiple sketches.

The simple logic of his model was (and still is!) very pleasing and, therefore, has been generally accepted since its initial publication. To test the model, from 1896 to 1898, the Funafuti

Coral Reef Boring Expedition of the Royal Society drilled down 340 m into the reefal crown of Funafuti Atoll (**Figure 1**), located in the tropical western Pacific; however, they did not reach the volcanic basement (Bonney 1904). It was only in the late 1940s and early 1950s, in preparation for nuclear testing on Bikini and Eniwetok Atolls (**Figure 1**), that basalt was finally encountered at the bottom of two boreholes drilled into Eniwetok Atoll, 1.3 km below sea level, overlain by Eocene neritic dolomitic limestone and younger reefal limestone (Ladd et al. 1953). In his geological note, Kuenen (1954) indicated that the basalt at the bottom of Eniwetok Atoll gave some support to Darwin's theory, though the atoll can be rationally explained only when significant ice-sheet-induced sea-level fluctuations are taken into consideration. However, one needs to remember that the basic concept of glaciations and our modern understanding of repeated high-amplitude sea-level fluctuations, with rates two to three orders of magnitude faster than the usual subsidence of volcanic edifices, were not known at the time Darwin developed his model.

Several geoscientists have proposed alternative models to Darwin's theory over the last 150 years (Daly 1915; Dana 1872; Davis 1928; Kuenen 1933, 1954; for a comprehensive description of the historical evolution of these models, see Davies 2011). Daly's (1915) marine-planation theory suggested that the successive stages described by Darwin are unrelated and result from differential wave erosion of unprotected shores during glacially lowered sea level, with barrier reefs forming on terraces and atolls forming on wave-leveled platforms during postglacial sea-level rise. As an alternative to the subsidence and planation theories, several authors, starting in the 1930s, proposed the antecedent karst model. This more realistic model, based on the then-new understanding of late Quaternary sea-level fluctuations, was initially developed by Kuenen (1933, 1954), improved by Hoffmeister & Ladd (1945, 1944), clearly and comprehensively explained (and nicely illustrated) by MacNeil (1954) (left side of **Figure 3**), and later improved once more by Purdy (1974) (right side of **Figure 3**), Purdy & Winterer (2001, 2006), Purdy & Gischler (2005), and Schlager & Purkis (2013).

The antecedent karst model takes into account, in addition to subsidence, the repeated late Quaternary high-amplitude (>100-m) sea-level fluctuations and relates the similarities of karst topography, formed during glacial periods of exposure when sea level had significantly fallen, to the development of the observed modern atoll morphology of a reef rim enclosing a central lagoon (**Figure 3**). A central depression surrounded by raised margins often forms during times of exposure, creating a template for future atoll formation through successive coralgal aggradation, which occurs preferentially along the margins of the system in successive periods of reflooding during sea-level transgressions and highstands (**Figure 3**). The duration of each late Quaternary sea-level highstand, on the order of 10,000–15,000 years (10–15 kyr), is not long enough for atoll lagoons to be filled up with carbonates produced within the lagoon or imported detritus from carbonate produced on the atoll rim (Gischler et al. 2008, Klostermann & Gischler 2015, Purdy & Gischler 2005).

Faros—the Maldivian name given to small atolls, usually only a couple of kilometers in size—are often found on the rims of larger atoll reefs or as lagoonal patch reefs (Agassiz 1902). Because of their small sizes and shallow lagoons, many faros, in only a few thousand years, become small, flat-topped banks once their lagoons were infilled with sediment, on top of which islands are sometime established (Kench 1998, Kench et al. 2015, Perry et al. 2013). For instance, the island of Malé, the capital of the Republic of Maldives, formed after the infilling of a faro that is part of the main rim of North Malé Atoll (Koksal 2014). If high sea level during Late Pleistocene interglacials had remained constant for a long period of time, as during the early and late Pliocene, then atolls may have evolved into flat-topped banks, as demonstrated through different computer models by Barrett & Webster (2012). Notably, such large flat-topped banks are common in the Maldives, as well as in the low latitudes of the western and central Pacific Ocean and southwest Indian

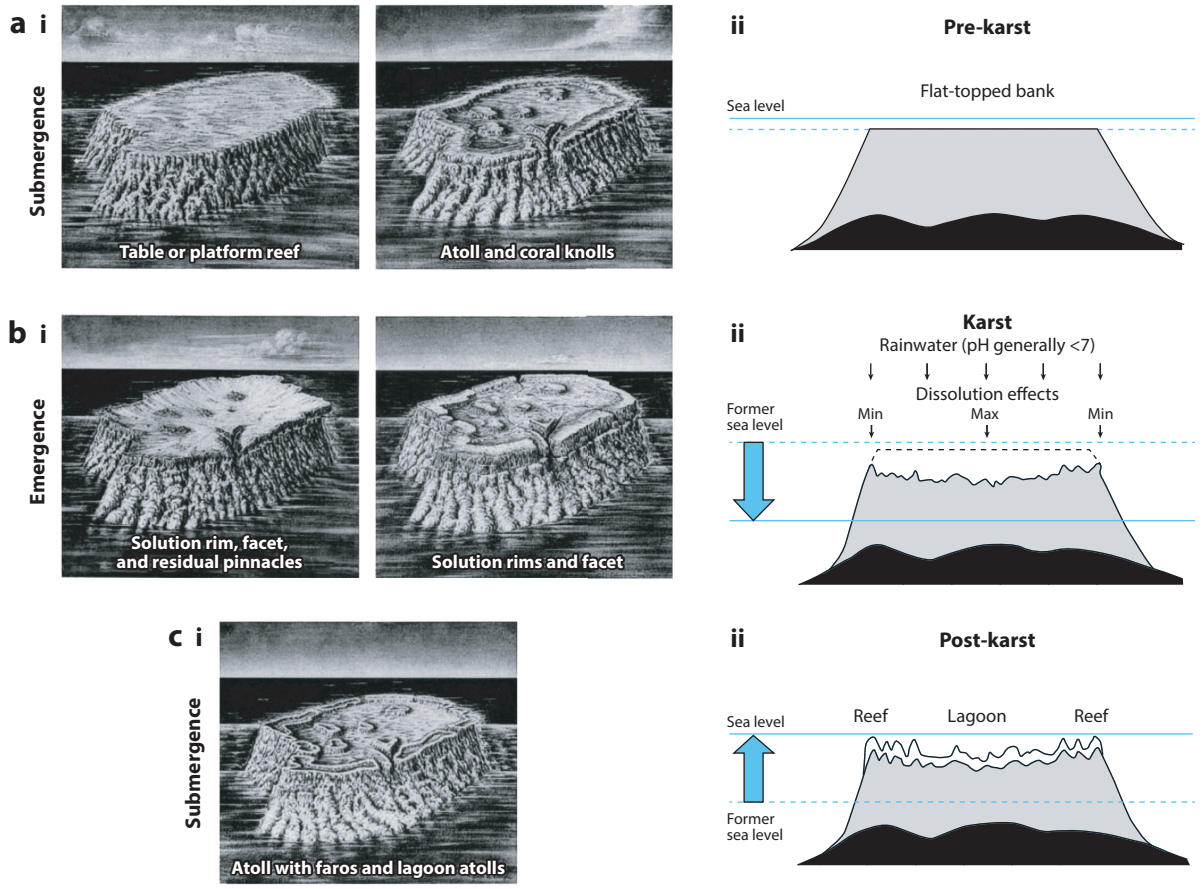

Figure 3

The antecedent karst model. The images on the left show the sequential steps in the model as proposed by MacNeil (1954); the illustrations on the right show modern atoll examples from Purdy (1974) to illustrate the link between reef shape and karst-induced antecedent morphology. The model includes three phases. (*a*) The first phase is active neritic carbonate production, starting with a table or platform reef and/or an initial atoll and coral knolls (subpanel *i*). This phase is illustrated as a flat-topped bank within the photic zone (subpanel *ii*). (*b*) In the second phase, the glacial lowering of sea level is larger than subsidence, resulting in subaerial emergence (subpanel *i*). This phase is illustrated as exposure and karstification of the bank/reef top (subpanel *ii*), with maximum dissolution in the center of the bank and minimum dissolution along its margins, creating a karstic central depression surrounded by raised solution rims. (*c*) Finally, the third phase is submergence (subpanel *i*). This phase is illustrated as a reflooding of the karstic topography by a deglacial rise of sea level in phase with subsidence (subpanel *ii*), with preferential coral-reef growth on the karstic external raised rim, where reef growth rates are optimum relative to the interior lagoon, resulting in an atoll. Reef passes across the atoll rim are inherited from glacial lowstand drainage breaches in the solution karstic rim. Subpanel *i* in all panels adapted from MacNeil (1954); subpanel *ii* in all panels adapted from Purdy (1974).

Ocean, throughout the geological record—for instance, in the early and middle Miocene and as recently as the late Pliocene, when the amplitudes of the sea-level fluctuations were small. On top of these late Pliocene banks, atolls ultimately grew in the late Quaternary, when the amplitude of late Quaternary sea-level fluctuations became unusually high and the interglacial intervals (when the sea level remained relatively constant) were very short. In spite of these well-proven alternative theories (particularly the antecedent karst model), the Darwin subsidence model has, surprisingly, withstood the test of time; even today, it is rarely questioned, is commonly taught in the Earth

science community at large, is included in most oceanography and Earth science textbooks, and is part of the definition of the term atoll on Wikipedia (2020).

In this review, we propose a comprehensive global model for modern atoll formation that combines the well-established patterns of ice-volume variations (and therefore sea-level fluctuations) over the last 5 million years (Myr) (i.e., Grant et al. 2019; Lisiecki & Raymo 2005; Miller et al. 2005, 2020; Spratt & Lisiecki 2016) with the observed evolution of Miocene/Pliocene flat-topped banks into numerous well-developed late Quaternary atolls. The model is based on convincing data sets from the Maldives Archipelago and Inner Sea acquired since the 1970s by the oil and gas industry (e.g., Elf Aquitaine and Royal Dutch Shell), dredging companies (e.g., Royal Boskalis Westminster N.V.), scientific drilling [e.g., Ocean Drilling Program (ODP) Leg 115 and International Ocean Discovery Program (IODP) Expedition 359], and several academic oceanographic research expeditions, such as the R/V *Meteor* research cruise in 2007 and a 2008 bathymetric multibeam survey around the island of Malé. The model is strengthened by drilling results from Mururoa and Funafuti Atolls in the tropical Pacific, interpretation testing through computer models, and new data sets from several expeditions in the Mozambique Channel in the southwest equatorial Indian Ocean, particularly Bassas da India Atoll (**Figure 1**).

2. SEA-LEVEL FLUCTUATIONS IN THE PLIO-QUATERNARY

The model proposed in this review is based on the well-established patterns of ice-volume variations (and therefore sea-level fluctuations) over the last 5 Myr (i.e., Grant et al. 2019; Lisiecki & Raymo 2005; Miller et al. 2005, 2020; Spratt & Lisiecki 2016). Therefore, we begin by summarizing the current knowledge of sea-level fluctuations in the Plio-Quaternary (last 5 Myr).

In a seminal article, Emiliani (1955) for the first time linked late Quaternary oxygen-isotope variations from planktic and deep benthic foraminifers to climate cycles driven by Milankovitch orbital forcing. Shackleton & Opdyke (1973) put forward the interpretation that variations in benthic and planktic oxygen isotopes were influenced by both temperature and ice volume and could therefore also be excellent records of cyclic sea-level fluctuations once the data were corrected for the temperature effect (Shackleton 1987). Since this pioneering research, high-resolution climate and ice-volume variations (and therefore sea-level records) have been extended much further back in time, particularly in the Plio-Quaternary. For that particular time interval, Lisiecki & Raymo (2005) developed a stack of numerous globally distributed benthic oxygen-isotope records, and Miller et al. (2005, 2020), after applying temperature corrections to some of those benthic oxygen-isotope records, established a sea-level curve for the last 5 Myr (**Figure 4*a***).

The Pliocene climate was warmer and more stable than today's climate; sea level overall was fluctuating by 20 m (or perhaps even 30 m) above and below the modern level (Miller et al. 2020) (**Figure 4*c***), with very-low-amplitude cycles, from the early to late Pliocene (Draut et al. 2003 and references therein). The late Pliocene—i.e., the 80-kyr-long (or even longer) warm interglacial interval from 3.27 and 3.19 Myr ago (Ma), encompassing most of the reverse Mammoth chron within the Gauss normal chron, often referred to as the mid-Pliocene warm period (MPWP) (Draut et al. 2003)—displays one of the last Pliocene very-low-amplitude cycles. This interglacial occurred during a very-low-eccentricity interval that promoted very-low-amplitude climate forcing at the 20-kyr precession frequency; climate and sea level remained surprisingly constant for four to six times longer than any of the middle and late Brunhes interglacial peaks (**Figure 4*b***). Planktic and benthic oxygen-isotope values during the MPWP remained quasi-unchanged, which is even more obvious when they are compared with the range of interglacial values during marine isotope stage (MIS) 11. That stage also occurred during a period of very low eccentricity, interpreted as an unusually warm interglacial that lasted twice as long as

any other mid-to-late Brunhes interglacials (Droxler et al. 2003; McManus et al. 1999, 2003) (**Figure 4*c*,*d***). The MPWP, an extended interglacial interval with unusually warm temperatures and low global ice volume, promoted relative stability on millennial timescales (Draut et al. 2003) (**Figure 4*d***).

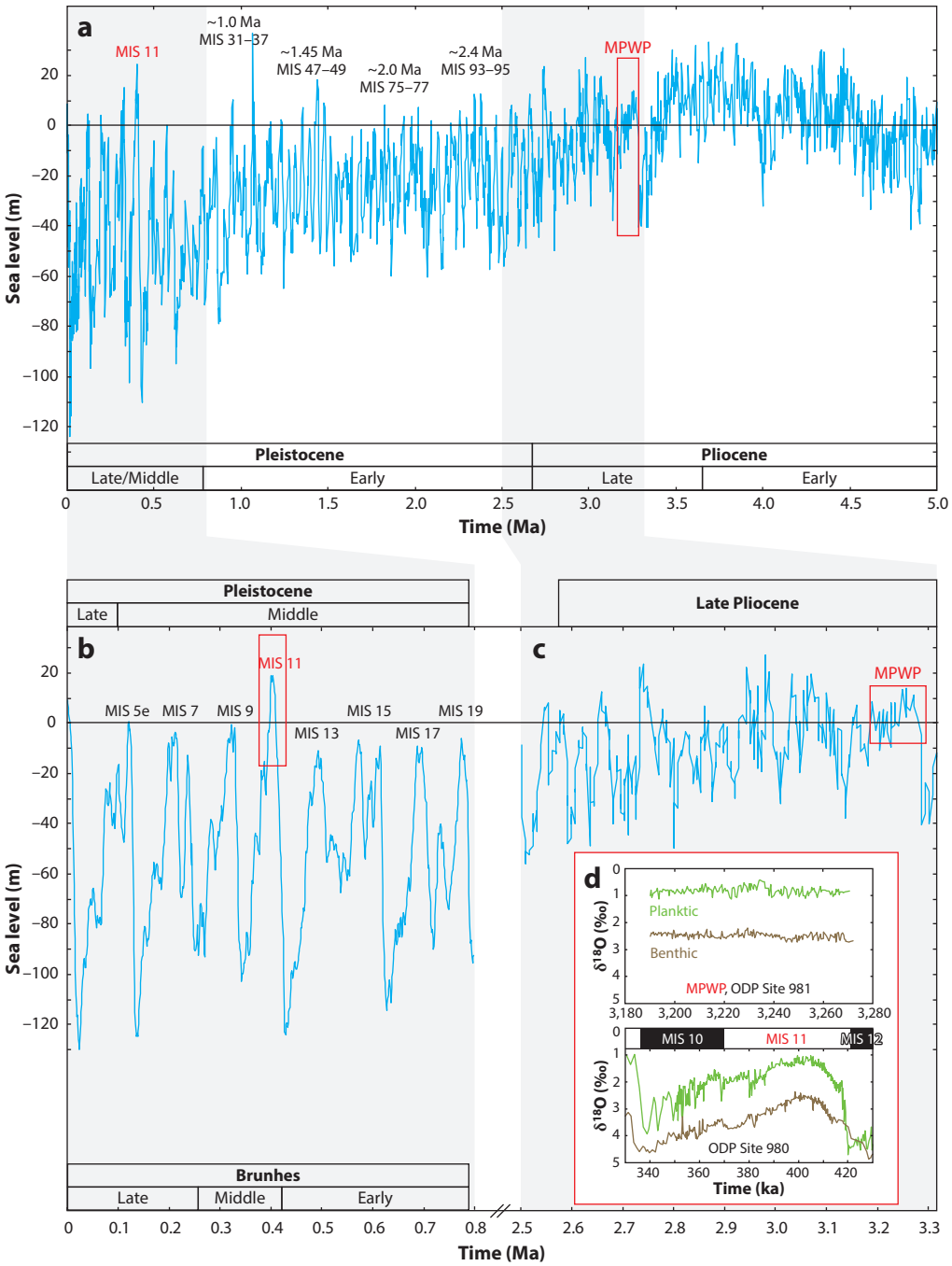

(Caption appears on following page)

Figure 4 (*Figure appears on preceding page*)

(*a–c*) Sea-level fluctuations over the past 5 Myr. Data are from Miller et al. (2020) (panels *a* and *c*) and Spratt & Lisiecki (2016) (panel *b*). (*d*) Planktic (*green lines*) and benthic (*brown lines*) oxygen-isotope records from ODP Sites 980 and 981 for the MPWP (*top*) and interglacial MIS 11 (*bottom*). Note how the benthic and planktic $\delta^{18}O$ interglacial values remain approximately constant for at least 80 kyr during the MPWP, while over the same time period, the benthic and planktic $\delta^{18}O$ interglacial values exhibit a full glacial cycle. Data are from Draut et al. (2003), McManus et al. (1999), and Oppo et al. (1998). Abbreviations: ka, thousand years ago; kyr, thousand years; Ma, million years ago; MIS, marine isotope stage; MPWP, mid-Pliocene warm period; Myr, million years; ODP, Ocean Drilling Program.

The climate deteriorated at the very end of the Pliocene and cooled enough to trigger the initiation of major Northern Hemisphere glaciations at approximately 2.6 Ma. During the Early Pleistocene, ending at the Brunhes–Matuyama boundary, which was also the beginning of MIS 19 (0.781 Ma), when the climate cooled with increasing intensity, the ice volume grew larger, and the sea level therefore fell accordingly. The climate was strongly influenced by obliquity on approximately 40-kyr cycles, with sea-level interglacial/glacial amplitudes on the order of 40–50 m. Four super-interglacial intervals at approximately 2.4 Ma (MIS 95–93), 2.0 Ma (MIS 77–75), 1.45 Ma (MIS 49–47), and 1.0 Ma (MIS 37–31) are well marked during the Early Pleistocene, when the sea level reached modern values or, in some instances, exceeded modern values (Miller et al. 2020) (**Figure 4*a***). At the beginning of the Brunhes, the climate continued to deteriorate but transited from 40-kyr obliquity to approximately 100-kyr eccentricity, driving high-amplitude interglacial/glacial cycles.

The Brunhes sea-level stack of Spratt & Lisiecki (2016) is shown in **Figure 4*b***. Ice volume reached a first maximum for the Plio-Quaternary during MIS 16, roughly equivalent to observed ice volume during the Last Glacial Maximum, when sea level globally fell to 125–135 m below the modern level (Yokoyama et al. 2018), following extreme glacials during MIS 12, 10, 6, and 2 (**Figure 4*b***). Because MIS 11 was an unusually warm and long interglacial, with high sea level estimated at approximately 6–13 m above the modern level (Droxler et al. 2003, Raymo & Mitrovica 2012), the deglaciation between MIS 12 and 11—referred to as Termination V, centered at approximately 430 kyr ago (ka)—is characterized by the highest amplitude in climate and ice-volume changes (and therefore sea-level changes) in the entire Plio-Quaternary, and even the full Cenozoic (**Figure 4*a***). The high amplitude of sea-level changes during the middle and late Brunhes is, therefore, quite unique. Because the climate was beating at a 100-kyr eccentricity frequency and a 20-kyr precession frequency, mid-to-late Brunhes peak interglacials lasted for approximately half of the 20-kyr precession beat during intervals of high eccentricity (MIS 9e, 16 kyr; MIS 7c, 11 kyr; MIS 5e, 16 kyr) and twice as long for the interglacial peaks (MIS 11c, 27 kyr; MIS 1, 12 kyr, but not complete yet) during intervals of low eccentricity (**Figure 4*b***).

3. THE MALDIVES

3.1. Modern Physiography

The Maldives Archipelago (**Figure 1**) is clearly visible from space and appears today as an 800-km-long series of north–south-oriented strings of more than 1,200 small atolls in the equatorial Indian Ocean (**Figure 5*a*,*b***). The numerous small faros are organized into 22 larger atolls that are tens of kilometers in diameter. The main lagoons of the larger atolls have water depths of 30–80 m, averaging 40–60 m (Naseer 2003), and increase in depth from north to south, a trend toward the equator, where the precipitation is highest (Purdy & Bertram 1993). The continuity of atoll rims is more prevalent in the south, whereas patch reefs and faros are more common in the north, influenced by stronger reversing monsoon winds and related ocean currents, in addition to

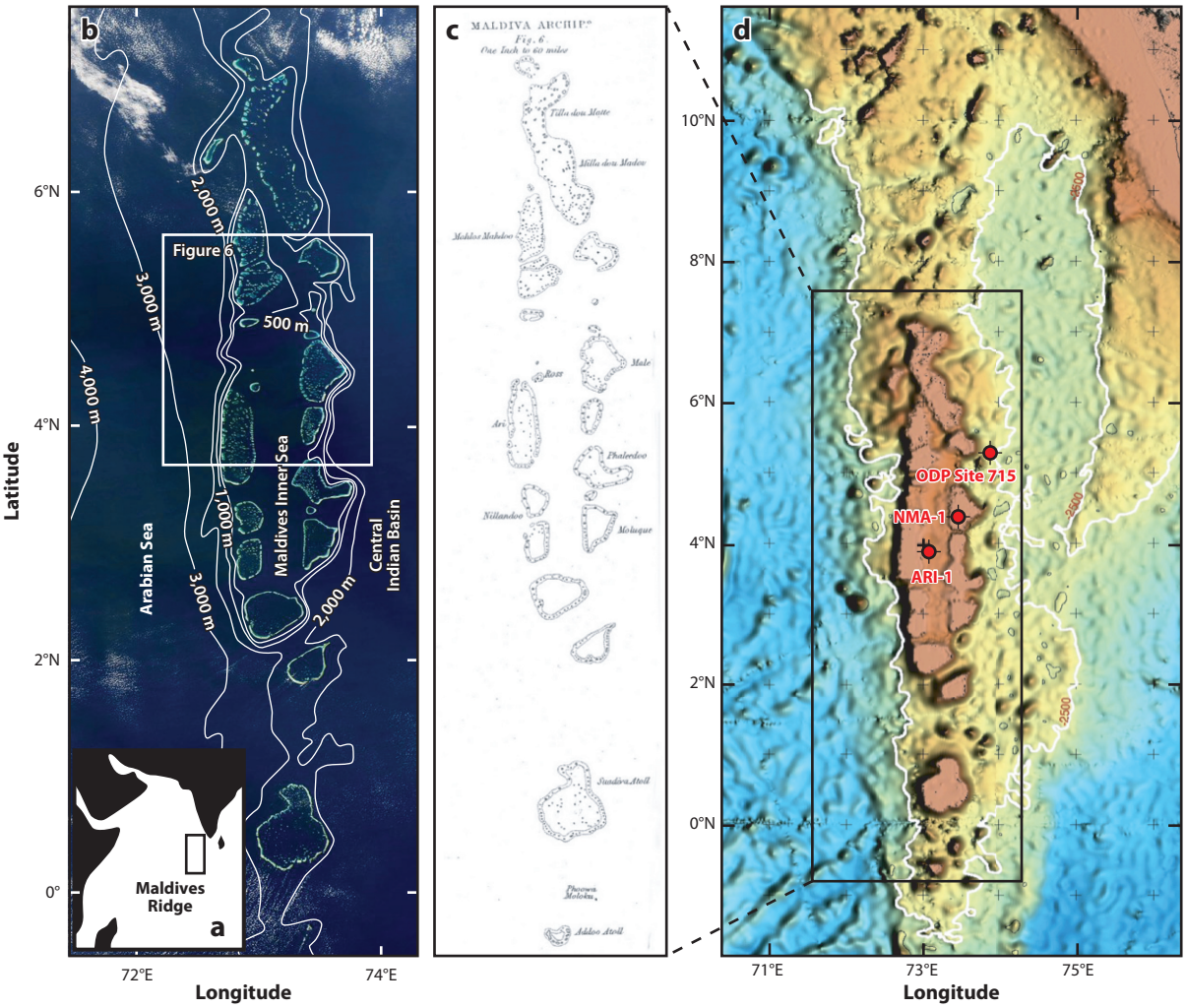

Figure 5

(*a*) Map showing the location of the Maldives Archipelago, southwest of the tip of India, in the equatorial low latitudes of Indian Ocean. (*b*) Satellite view of the Maldives Archipelago (with bathymetric contours in meters), illustrating its central double chain of atolls bordering the Maldives Inner Sea. (*c*) Map of the Maldives Archipelago from Darwin (1842). Note how similar this map is to the satellite view shown in panel *b*. (*d*) Map of radar-altimeter-derived free-air gravity anomalies centered on the Maldives Archipelago, where the bluish color indicates abyssal depths greater than 2,500 m and reddish-brown indicates water depths less than 2,000 m. The free-air gravity anomaly derivation is based on algorithms developed by Smith & Sandwell (1997). The volcanic plateau top, on which the Maldives neritic carbonate system was established about 55–57 Ma, ranges in water depths between 2,000 and 2,500 m, shown roughly in orange, and was drilled and recovered at the bottom of the ARI-1 and NMA-1 industry wells, in addition to ODP Site 715 (shown on the map). Abbreviations: Ma, million years ago; ODP, Ocean Drilling Program. Panel *b* courtesy of NASA; panel *c* adapted from Darwin (1842); panel *d* courtesy of ConocoPhillips.

more frequent storms (Kench 2011). In the central part of the archipelago, the large atolls form two parallel, relatively continuous north–south chains surrounding an internal basin, the Inner Sea, with water depths of up to 600 m. This specific general organization of the larger atolls into two parallel north–south chains was already well mapped by the British Royal Navy in Darwin's time, as shown by one of the figures included in his 1842 publication (**Figure 5*c***). The similarities

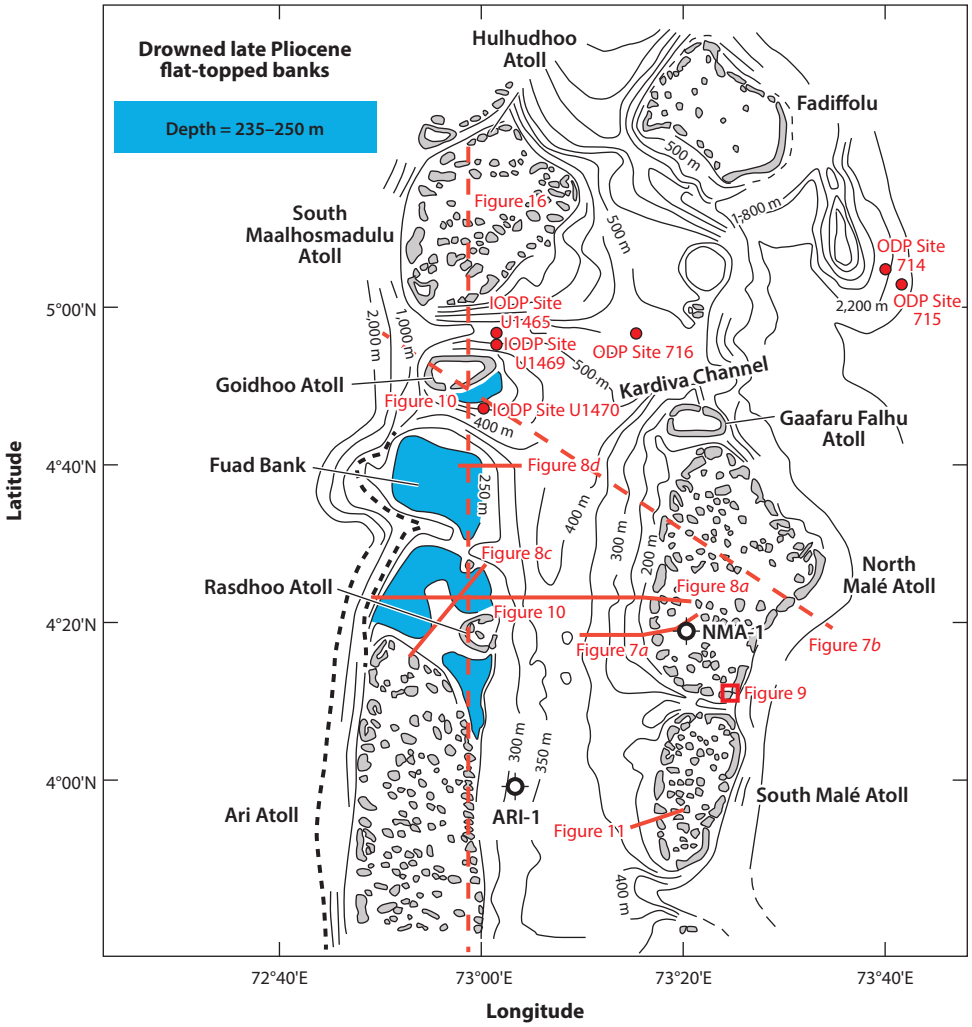

Figure 6

Bathymetric map showing the northern part of the central double chain of atolls bordering the Maldives Inner Sea. The locations of existing industry wells, ODP/IODP drill sites, and places shown in some of the other figures in this review are indicated. Notice that the western chain of atolls is not perfectly continuous and that the segment along which the atolls are missing corresponds to drowned or partially drowned flat-topped banks (*blue areas*). Abbreviations: IODP, International Ocean Discovery Program; ODP, Ocean Drilling Program.

between the satellite image (**Figure 5*b***) and Darwin's figure (**Figure 5*c***) are quite astonishing and attest of the great mapping capabilities of the British Royal Navy in the early 1800s.

A careful inspection of **Figure 5*a*,*b*** reveals that the western chain of atolls is interrupted on the northwest margin of the Inner Sea, between Ari and Rasdhoo Atolls in the south and Goidhoo Atoll in the north, by a gap of half a degree of latitude (**Figures 5** and **6**) along which atolls do not exist. The bathymetric map of the central part of the Inner Sea clearly reveals that, where the atolls were expected to be, there is instead a series of three drowned flat-topped banks (**Figure 6**), which include the area north of Ari Atoll; the central area of the gap, known as Fuad Bank; and

the flat terrace southeast of Goidhoo Atoll, all of which fall in a narrow range of water depths between 230 and 250 m (**Figure 6**).

The Republic of Maldives consists of many small islands that are scattered throughout the archipelago and are barely observable on Google Maps, with an average elevation of 1.5 m. They represent a tiny fraction of the extensive 2–3-km-thick submerged Maldivian carbonate megaplatform, particularly in terms of their surface area and overall thickness (Aubert & Droxler 1992, 1996; Belopolsky & Droxler 2003, 2004; Purdy & Bertram 1993) (**Figure 5*d***). Importantly, unlike other large carbonate systems along continental margins, such as the Great Barrier Reef and the Bahamas–Florida platforms, the Maldivian carbonate megaplatform has grown, since approximately 55 Ma, on top of a slowly subsiding, initially exposed volcanic plateau (yellow areas in **Figure 5*d***) that is much larger than the Maldivian carbonate megaplatform (reddish-brown areas in **Figure 5*d***). The volcanic plateau was established on oceanic crust and is part of the hot-spot track of the island of Réunion (Duncan & Hargraves 1990) (**Figure 5*d***).

3.2. Long-Term Geological Evolution of the Maldives

Hydrocarbon exploration in the Maldives, initiated by Elf Aquitaine in the early 1970s, has provided some excellent data sets that were made available for academic research. Several two-dimensional seismic surveys were made both in the Inner Sea and in the atoll lagoons. In 1976, Elf Aquitaine drilled an exploration well, NMA-1, inside the North Malé Atoll lagoon, northwest of the island of Malé (**Figures 5*d***, **6**, and **7**). The well penetrated a 2,106-m-thick carbonate sedimentary succession laid down from the Eocene to recent times before drilling into 116 m of weathered Paleocene basalts, which the argon–argon method dated to 55 Ma (Duncan & Hargraves 1990) (**Figure 7**). The interpretation of these early data sets by Aubert & Droxler (1992, 1996) and Purdy & Bertram (1993) provided the first framework for the overall evolution of the Maldivian carbonate megaplatform. In the late 1980s, Royal Dutch Shell acquired a relatively dense (1–2-km spacing), 6,000-km regular seismic grid spanning the entire Inner Sea and covering an area of 275 km by 50 km. Shell drilled the ARI-1 well at a water depth of 300 m in the Inner Sea, southeast of Ari Atoll (**Figures 5**, **6**, and **7*b***). This well reached the volcanic plateau top at approximately 3.3 km (Aubert & Droxler 1996; Belopolsky & Droxler 2003, 2004). Because the basalts in ARI-1 were highly altered, radiometric age dating of the basalt was not successful.

In 1987, the ODP drilled three sites in the Maldives. ODP Site 716 was drilled at a water depth of 500 m in the northern part of the Inner Sea; this site recovered 262 m of oozes and chalks from the Pleistocene to the late Miocene (Backman & Duncan 1988a) and is a good complement to the ARI-1 well drilled farther south in the Inner Sea, in which the top 250 m of the sedimentary sequence was not recovered. Site 716 fully recovered continuous sedimentary section that covers the last 7 Myr (Backman & Duncan 1988b) and helps to tie the well stratigraphy to the main reflectors identified in the seismic data set (Aubert & Droxler 1996; Belopolsky & Droxler 2003, 2004). ODP Sites 714 and 715 were drilled at the toe of the Maldivian carbonate escarpment in 2,041 and 2,262 m of water depth, respectively, approximately 40 km southwest of Fadiffolu Atoll (**Figures 5*d***, **6**, and **7*b***). The basalt–shallow-water limestone (late early Eocene in age; Nicora & Premoli Silva 1990) transition was recovered at Site 715, 210 m below the seafloor, or 2,472 m below sea level. The basalt was dated by the argon–argon method to 57 Ma and was recognized to have been altered while exposed on land (Duncan & Hargraves 1990). Site 714 recovered some Miocene periplatform chalks without reaching the basaltic plateau (Backman & Duncan 1988a).

New data sets (multibeam maps, multichannel high-resolution seismic data using a wide range of high-frequency energy sources, and coring) were acquired during the 2007 R/V *Meteor* research cruise (Betzler et al. 2009; Fürstenau et al. 2010; Lüdmann et al. 2013, 2018). IODP Expedition

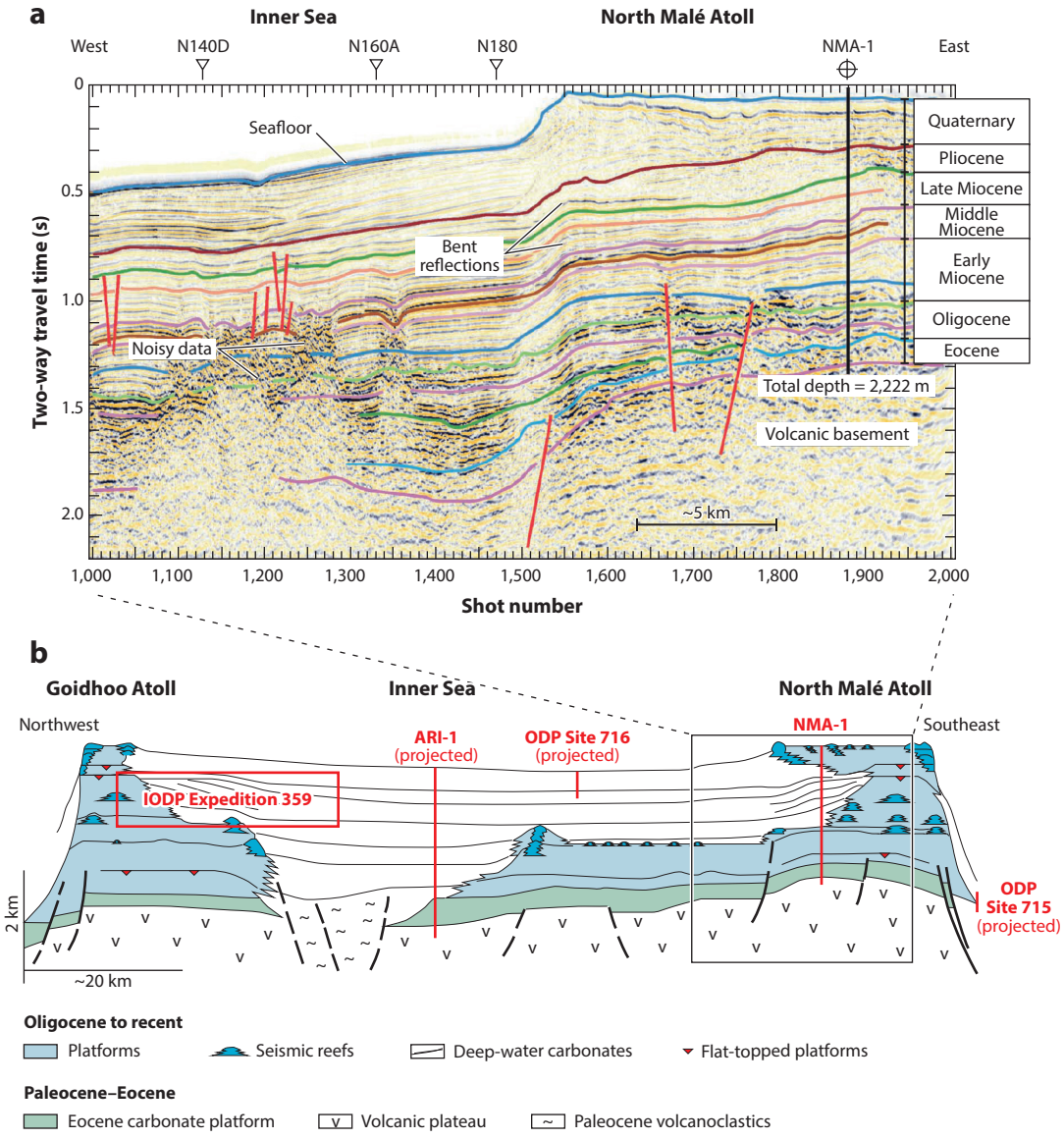

Figure 7

(*a*) Royal Dutch Shell seismic line through the southwestern North Malé Atoll margin and the NMA-1 well. (*b*) Schematic cross section through the full width of the Maldives Archipelago, along which existing well and drill sites are projected. Notice that Goidhoo and North Malé Atolls correspond only to the most recent part of the 55-Myr evolution of the Maldivian carbonate mega-platform. Following a major partial drowning of the Oligocene mega-platform top, the platform evolved into a giant atoll-like structure in which both ocean-facing margins continued to grow, enclosing the Inner Sea, and evolved into the double chains of atolls characteristic of the Maldives Archipelago as we know it today. The Inner Sea constitutes the interior of the "empty bucket," named by Schlager & Purkis (2013). Abbreviations: IODP, International Ocean Discovery Program; Myr, million years; ODP, Ocean Drilling Program. Panel *a* adapted from Belopolsky & Droxler (2003, 2004); panel *b* adapted from Belopolsky & Droxler (2004).

359 recovered two transects of drill sites directly north and south of Goidhoo Atoll (Betzler et al. 2016a, 2017). Three sites from Expedition 359—U1465, U1469, and U1470 (**Figure 6**)—reached the top or drilled the Miocene flat-topped platform. As interpreted in early studies by Aubert & Droxler (1992, 1996) and Belopolsky & Droxler (2003, 2004), the drilling results confirmed that Ghoidoo Atoll is the remnant, through segmentation and back stepping, of a much larger flat-topped platform that partially drowned in the middle Miocene (approximately 13 Ma) at depths of 575 m and 650 m below modern sea level (Betzler et al. 2016a, Lüdmann et al. 2018).

Aubert & Droxler (1992, 1996), Purdy & Bertram (1993), and Belopolsky & Droxler (2003, 2004) documented the long-term evolution of the Maldivian carbonate megaplatform over the past 55–57 Myr. Interpretation of the seismic profiles showed that a series of long, deep grabens oriented north-northeast–south-southwest crosscut the volcanic plateau, and these grabens are clearly imaged in a three-dimensional model by Belopolsky & Droxler (2003, 2004). Eocene carbonate banks became established on topographic highs of the faulted volcanic plateau when it subsided below sea level (**Figure 7*b***), and movement along the graben faults continued until the late Oligocene. The 55-Myr evolution of the 2–3-km-thick carbonate megaplatform is quite complex, with a long interval of vertical growth during the Eocene and Oligocene, followed by an interval of massive drowning at the end of the Oligocene and the beginning of the early Miocene (**Figure 7*a*,*b***). IODP Expedition 359 twice drilled a 100-m-thick sequence of interbedded organic-rich sediment and pelagic carbonates that were deposited in the late Oligocene and early Miocene when the proto–Inner Sea basin became anoxic (Swart et al. 2019), which would explain the massive drowning of the Oligocene megaplatform. The influence of the volcanic basement morphology remained a factor controlling the distribution of shallow carbonate banks only through the very first part of the early Miocene, after which its influence was muted. Consequently, modern atoll occurrence and development are clearly unrelated to the volcanic basement. Below, we demonstrate that the modern atolls are only the final phase of the Neogene and Quaternary evolution of the Maldivian carbonate megaplatform (**Figures 7** and **8**).

During the early Miocene (N1 and N2 in **Figure 8*b*** and in **Figure 11*b–d*** below; see Section 3.4), the shallow carbonate system, which is much more restricted in surface areas relative to the underlying Oligocene platform, continued to grow in a vertically restricted way to both ocean margins of the Maldivian carbonate megaplatform and then became partially exposed during the late middle Miocene (N3) at approximately 13 Ma (Betzler et al. 2016a, 2017) (**Figures 7** and **8*a***). Strong currents, related to the abrupt onset of the monsoonal regime (Betzler et al. 2016b)—one of the factors with related strong ocean currents (Owen et al. 2011)—is still highly influencing the Maldives Archipelago today (Betzler et al. 2009) and triggered the initial segmentation of the late middle Miocene flat-topped platform. A segment of this platform has now become the Goidhoo Atoll platform. In the late middle Miocene and late Miocene, the carbonate system grew laterally only through bidirectional progradations that partially filled the Inner Sea (Aubert & Droxler 1996; Belopolsky & Droxler 2003, 2004; Lüdmann et al. 2013, 2018) (**Figure 7*b***), which since IODP Expedition 359 have been interpreted as thick carbonate delta drifts (Betzler et al. 2016a; Lüdmann et al. 2013, 2018).

Full reflooding of the external margins of the carbonate megaplatform, which are now segmented, occurred in the late Miocene (N4) and Pliocene (N5) (**Figures 7** and **8**). The platforms that remained along both the western and eastern margins of the Maldivian carbonate system evolved into systematic and characteristic segmented flat-topped banks, such as the late Pliocene (N5) partially drowned banks in the northern part of Ari Atoll and southeastern part of Goidhoo Atoll (**Figures 6** and **8*a–c***), in addition to contemporaneous flat-topped banks imaged under North and South Malé Atolls (**Figures 7*a*** and **8*a*,*b***). Fuad Bank corresponds to a fully drowned late Pliocene (N5) carbonate flat-topped platform (**Figure 8*d***) on top of which an atoll could not

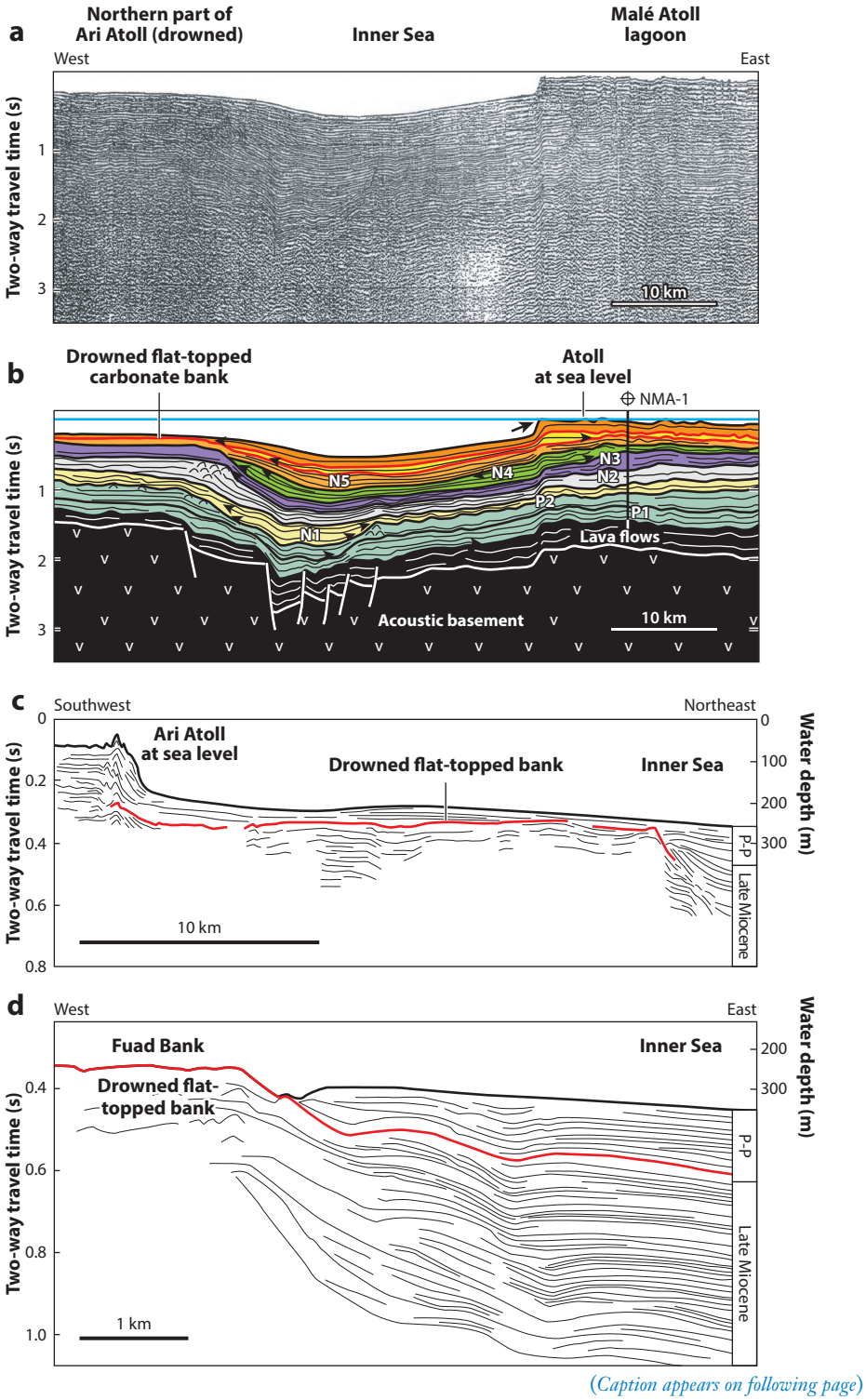

(Caption appears on following page)

Figure 8 (*Figure appears on preceding page*)

(*a*,*b*) Seismic line (shown in panel *a* and interpreted in panel *b*) crossing almost the entire carbonate megaplatform, from the south of the active Malé Atoll to the drowned Pliocene flat-topped bank of North Ari Atoll, lying at water depths of 235–250 m. The P and N numbers are Paleogene and Neogene seismic units, respectively, as defined by Aubert & Droxler (1996). (*c*) Seismic line crossing the northern part of Ari Atoll, showing the transition from its Pliocene drowned flat-topped bank, lying at water depths of 235–250 m, and the live part of Ari Atoll. (*d*) Seismic line crossing the eastern part of Fuad Bank, located between Ari and Maalhosmadulu Atolls, on a Pliocene flat-topped bank, also lying at water depths of 235–250 m, although completely drowned. The locations of all three seismic lines are shown in **Figure 6**. Abbreviation: P-P, Plio-Pleistocene. Panels *a* and *b* adapted from Aubert & Droxler (1996); panel *c* adapted from Betzler et al. (2009); panel *d* adapted from Lüdmann et al. (2013).

develop. In seismic lines crossing some of the modern atoll margins facing the Inner Sea, it appears that the modern atolls have grown on older flat-topped banks. This is illustrated on the seismic line in **Figure 7*a***, where the younger red reflector corresponds to a late Pliocene flat-topped bank underlying the late Quaternary North Malé Atoll.

In summary, the modern atolls in the Maldives Archipelago are clearly part of the final mid-to-late Brunhes phase of the evolution of the Maldivian megaplatform since the Eocene. Their atoll morphologies therefore developed completely independently of the underlying volcanic basement.

3.3. The Evolution of Modern Atolls During the Past 20,000 Years

Lines of evidence for the exposure of modern atolls in the recent past are obvious on the atoll upper slopes and their lagoon floors. In 2008, a high-resolution multibeam mapping survey was conducted around the island of Malé (located on the southeast rim of North Malé Atoll, as shown in **Figures 6** and **9*a***). This survey imaged the likely location of the Last Glacial Maximum coastline, observed at approximately 125 m below sea level, where a change in slope dip occurs (**Figure 9*b***). It also imaged a series of steps along the slope that mimicked the well-established stepwise/punctuated sea-level rise (meltwater pulses) during the last deglaciation (Rovere et al. 2018) (**Figure 9*b***). Similar submerged reef terraces or steps were imaged during the 2007 multibeam survey south of Rasdhoo Atoll and north of Ari Atoll (Fürstenau et al. 2010). Finally, the 2008 survey also imaged a well-developed paleo-karst morphology on the North Malé Atoll lagoon floor at a water depth of 40–60 m, where Holocene sediments are continuously removed by strong currents that flow through Vaadhoo Channel and reverse themselves during the annual monsoon (Owen et al. 2011) (**Figure 9*c***).

A 17-m-deep borehole known as Core 1, drilled on the western rim of Rasdhoo Atoll (**Figure 10*d***), clearly illustrates the stacking of a 13.5-m-thick MIS 1 Holocene interglacial reef unit dated as far back as 8.2 ka (radiocarbon age) (**Figure 10*f***). The Holocene reefal unit rests on top of the previous interglacial highstand unit MIS 5e, dated at 136.9 ka (uranium–thorium age) (**Figure 10*f***). Both units are separated by a clear exposure horizon that therefore represents more than 100 kyr of exposure associated with the end of interglacial MIS 5 and the MIS 4–2 glacial lowstand (Gischler et al. 2008). Kench et al. (2009) reported a similar succession drilled on the Hulhudhoo reef flat (**Figure 6**) on South Maalhosmadulu Atoll, where the last interglacial reef, dated at 122 ± 7 ka (uranium–thorium age), was recovered at 14 m below sea level. The earliest reef establishment on top of the last exposed karst surface was dated to 8.1 cal kyr BP; the reef grew steadily until 6.5 cal kyr BP and then grew at a decreasing rate for the next 2 kyr, when sea level had reached or even exceeded by a couple of meters the modern level, at approximately 4.5 cal kyr BP. In both locations, the marginal reefs grew in a keep-up mode at a rate of approximately 15 m/kyr. The incomplete sediment infilling of Rasdhoo Atoll lagoon is typified by a thin (∼4 m) sediment

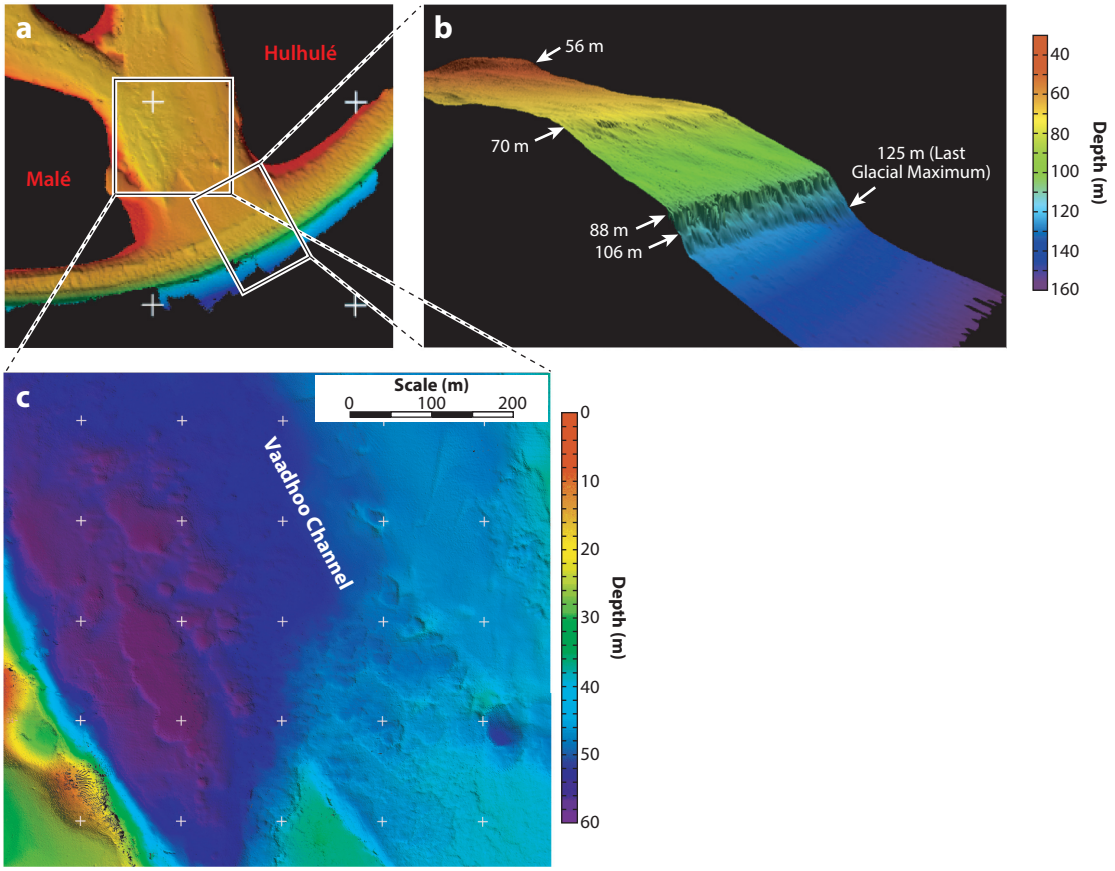

Figure 9

(*a*) Bathymetric map of the southern extremity of North Malé Atoll, between the islands of Malé and Hulhulé. (*b*) Upper-slope morphology in a three-dimensional map created in collaboration with Professor David Naar of the University of South Florida. This morphology reveals multiple reef terraces, which have been interpreted as the expression of reef back stepping during the last deglacial sea-level rise (Rovere et al. 2018). (*c*) Bathymetric map showing the channel seafloor, which lies at water depths of 40–60 m, in a series of enclosed and unfilled round or oval depressions. These depressions are typical in karst dissolution morphologies, illustrating that the North Malé Atoll lagoon floor was exposed when the sea level was below 40–60 m. The location of this bathymetric data set is shown in **Figure 6**.

cover, Middle to Late Holocene in age, that rests on top of Early Holocene (~10 ka) peat and paleosoil deposits (**Figure 10*e***).

The available seismic survey and cores in the Goidhoo Atoll lagoon (**Figure 10*a–c***) clearly show the Late Pleistocene rugged topography, which is typical of karstic morphology. The deepest central lagoon (today ~40 m in depth) has been partially buried by more than 6 m of Holocene sediment (maximum thickness of 15 m), and the Holocene sedimentary fill buries the karstic rough surface and creates the smooth seafloor topography observed today. The deepest depressions in the karstic Pleistocene surface reach approximately 55 m below sea level, a water depth similar to those of the unfilled karstic depressions observed on the seafloor of the North Malé Atoll lagoon (**Figure 9**). Following the seismic acquisition, four cores were collected in the Goidhoo Atoll lagoon (**Figure 10*a***). Whitish, soft, very silty carbonate mud was recovered in three cores from the middle of this lagoon: GD1 (4.4 m), GD2 (4.6 m), and GD3 (4.5 m). Core GD6, located in

a proximal location just north of the southern Goidhoo Atoll rim, recovered 4.3 m of carbonate sediment. This core illustrates the partial coarsening and then fining upward infill of the lagoon; the bottom 10 cm consists of whitish fine and medium sand, the interval from 4.3 to 3.7 m is composed of whitish, fine to coarse, silty, sandy gravel with cobbles (gravel and cobbles consist of coral, shells, shell fragments, and cemented sand), and the upper 3.7 m is made of whitish, soft, very silty mud (slightly gravelly, with shell fragments).

These studies in Rasdhoo, Hulhudhoo, and Goidhoo Atolls demonstrate that, in the Holocene, the differences between vertical reef growth rates (an average of 7.25 m/kyr and as high as 15 m/kyr) and lagoonal sediment accumulation rates (0.68 m/kyr) explain why atolls display their

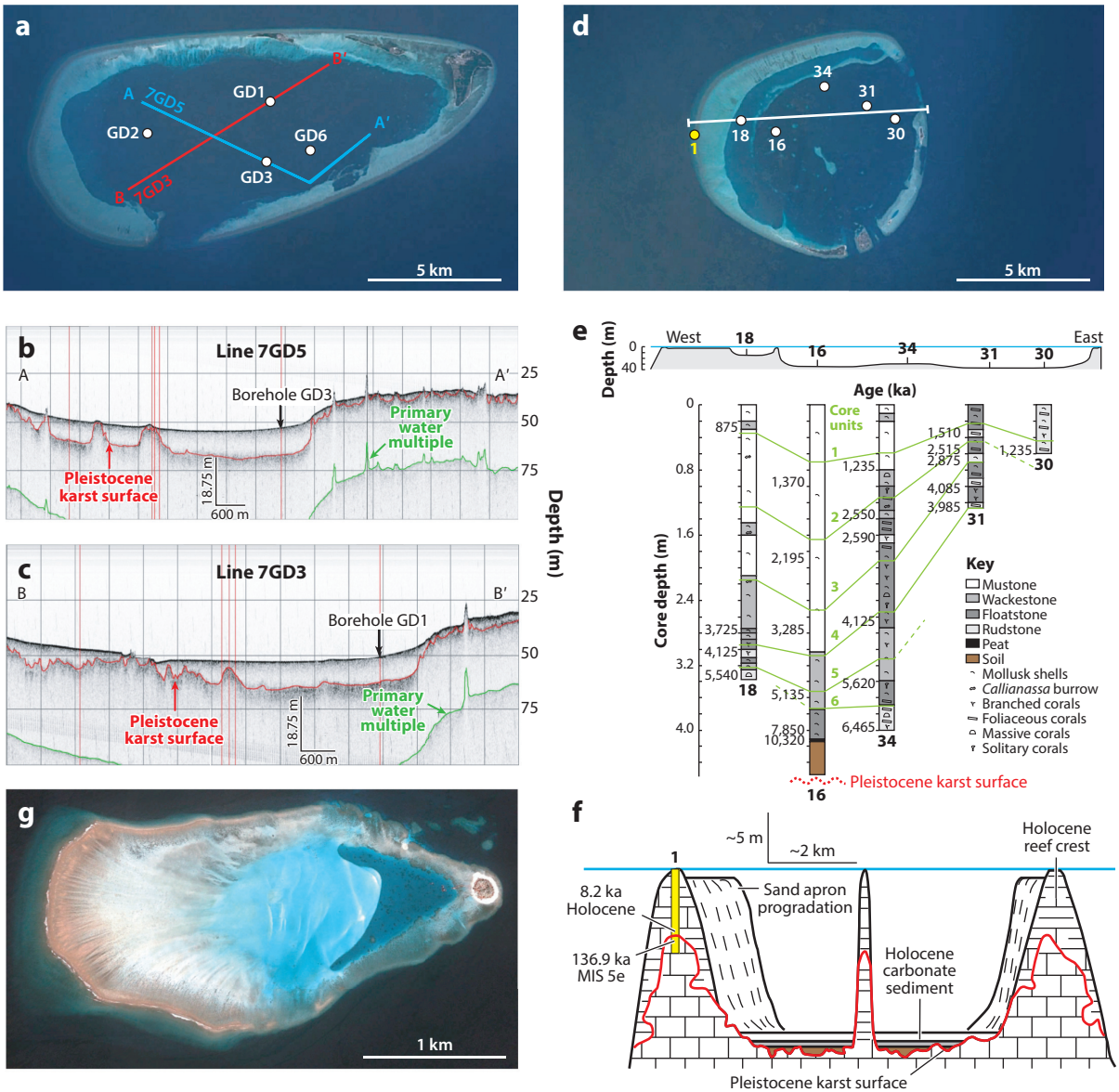

(Caption appears on following page)

Figure 10 (*Figure appears on preceding page*)

(*a*) Satellite image of Goidhoo Atoll, showing the locations of boreholes and two seismic lines illustrated in panels *b* and *c*. (*b*,*c*) Seismic profiles acquired in the Goidhoo Atoll lagoon, imaging the Holocene sediment cover above a karstified Pleistocene surface (*red line*). (*d*) Satellite image of Rasdhoo Atoll, showing the locations of sediment cores retrieved in the lagoon (data from Klostermann & Gischler 2015) and presented in panel *e*, as well as Core 1 (*yellow*), which was drilled on the reef crest (Gischler et al. 2008) and is presented in panel *f*. (*e*) Transect of sediment cores through central Rasdhoo Atoll lagoon. These data confirm that the substrate of the modern lagoon (below the Holocene sediments, which have a maximum thickness of approximately 4 m) is characterized by the presence of karst and soil deposition (see panel *f*). (*f*) Schematic cross section of Rasdhoo Atoll, showing the Holocene reef growth and lagoonal sediment fill. As in the Ari Atoll faro shown in panel *g*, the Rasdhoo Atoll lagoon is being filled in, above the karstified Pleistocene surface, mostly by sediment progradation from the windward atoll rim, where the wave energy and neritic carbonate production are at their highest. The last interglacial (MIS 5e) corals dated at 136.9 ka were reached by drilling in Core 1 (*yellow*), on the western reef crest, and are directly overlain by early Holocene corals dated at 8.2 ka. Both coral accumulations are separated by an approximately 100-kyr-long unconformity, representing an exposure horizon and karstification. (*g*) Google Earth satellite image of a faro located on the western rim of Ari Atoll. Note how the faro lagoon is being filled from west to east by neritic carbonate that is being produced mainly along the western rim, where wave energy is optimum, and exported toward the lagoon. Abbreviations: ka, thousand years ago; MIS, marine isotope stage. Panel *e* adapted from Klostermann & Gischler (2015); panel *f* adapted from Gischler et al. (2008) and Klostermann & Gischler (2015).

typical empty-bucket morphology, creating their own unfilled accommodation within their interiors during deglacial sea-level rise. Since 6.5 ka, sea level has remained relatively constant in the Maldives, whereas the sedimentation rates in the lagoons have increased. During a sea-level stillstand, sand aprons behind the reef flats formed on both sides of the lagoons and initiated their progradation into the lagoons while infilling the lagoons themselves (**Figure 10*f***). The windward or high-energy margin reef sand apron is more developed than that on the lee side of the reefal margin. The asymmetry of the atoll-lagoon filling from its high-energy side is illustrated in a faro from the western margin of Ari Atoll (left side of **Figure 10*g***, where waves are breaking on the reef crest). Because sea level remained approximately constant during the MPWP interval, most likely fluctuating within a few meters for at least approximately 80 kyr (**Figure 4*c*,*d***), lagoons of existing atolls during the Pliocene would likely have been filled up, resulting in the common flat-topped banks observed in the late Pliocene.

3.4. Overall Evolution During the Neogene and Quaternary

Interpretation of seismic profiles across the modern atoll margins of the Maldives, in the context of fairly well-established global ice-volume variability and sea-level fluctuations in the past 5 Myr (Lisiecki & Raymo 2005; Miller et al. 2005, 2020), illustrates that, for instance, along the western margin of South Malé Atoll (**Figure 11**), a shift took place from middle Miocene–Pliocene sigmoid lateral margin progradation of flat-topped carbonate banks (**Figure 11*a***) to late Quaternary bank-top vertical aggradation that evolved into the modern atoll physiography (**Figure 11*c***). This well-marked transition is first illustrated by a regionally observed downward shift of the depositional system initiated at approximately 2.5 Ma. This downward shift of onlap is explained by an overall sea-level fall during the Early Pleistocene that was tied to the onset and successive expansions of major continental ice sheets in the Northern Hemisphere (**Figure 11*b***). The Pliocene bank tops remained exposed most of the time for approximately 2 Myr and then were successively flooded and exposed by a series of five sea-level rises and falls with amplitudes of more than 120 m during the mid-to-late Brunhes (**Figure 11*c*,*e***). The exposed banks might have been briefly reflooded several times in the Early Pleistocene at approximately 2.4 Ma (MIS 95–93), 2.0 Ma (MIS 77–75), 1.5 Ma (MIS 49–47), and 1.0 Ma (MIS 37–31) (**Figure 11*e***). The initial karst topography during the series of exposures, which were particularly enhanced during the latest part of the Early Pleistocene and the early Brunhes (when the glacial–interglacial frequency evolved from 40- to 100-kyr cycles, with ice volumes reaching their initial maxima

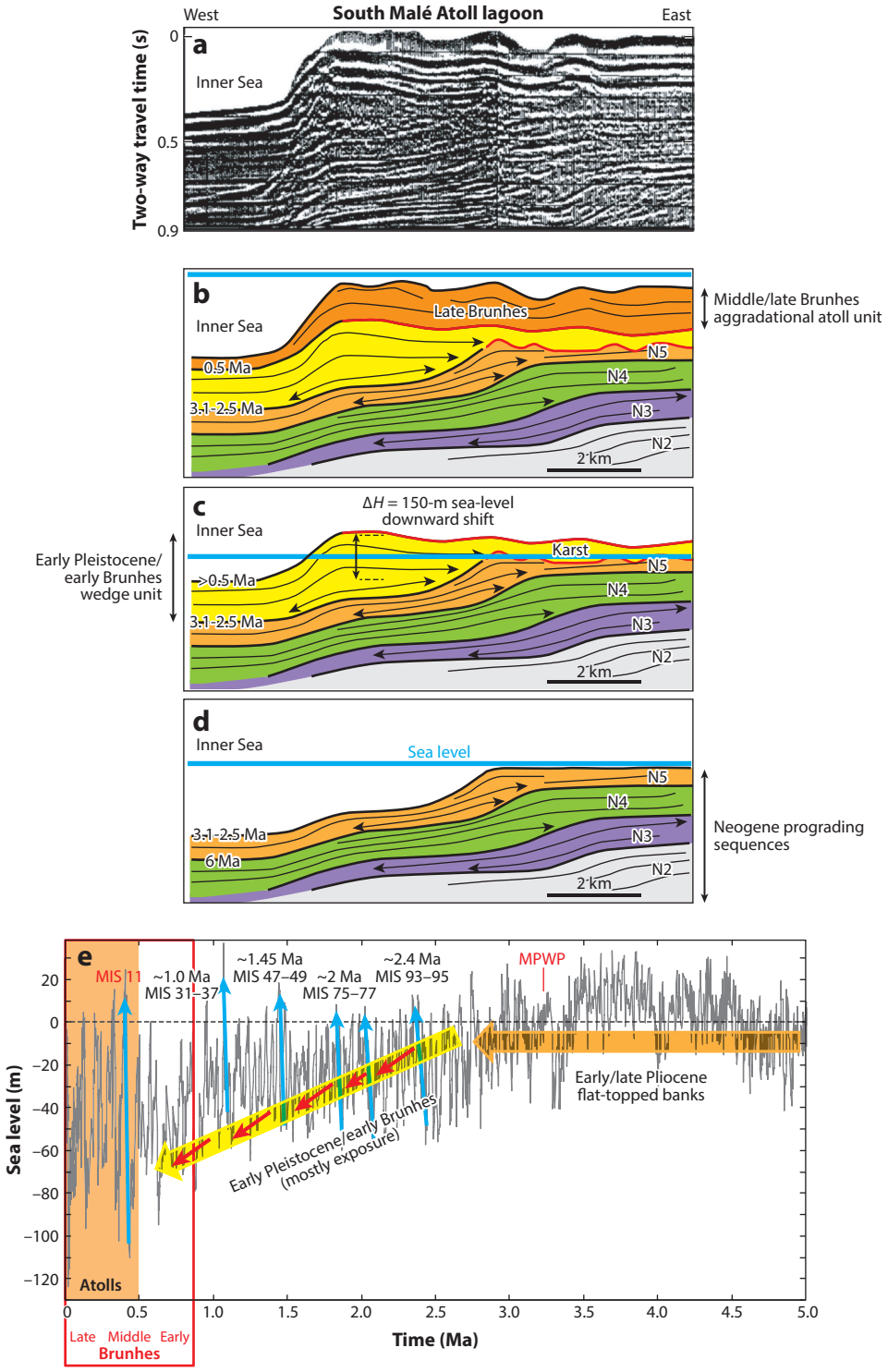

(*Caption appears on following page*)

Figure 11 (*Figure appears on preceding page*)

(*a*) Elf Aquitaine seismic line crossing the South Malé Atoll western margin (shown in panel *a* and interpreted in panels *b–d*). The location of this seismic line is shown in **Figure 6**. (*b–d*) Model showing how flat-topped banks in the late. Pliocene (panel *d*) formed during a long interval of high sea level with low-amplitude fluctuations (panel *e*). The flat-topped bank was first exposed during the very end of the Pliocene, then during the Early Pleistocene and the early Brunhes (panel *c*), which was a long interval of systematically falling sea level with the formation of karsts (panel *e*), with a short time of possible reflooding during four super-interglacial intervals: MIS 95–93, 77–75, 49–47, and 37–31. During the middle/late Brunhes, when modern atolls formed (panel *b*), a time of five well-developed 100-kyr glacial/interglacial cycles, the karstified late Pliocene flat-topped banks were periodically reflooded during MIS 11, 9, 7, 5, and 1 and exposed during the intervening glacial (panel *e*). The N numbers are Neogene seismic units, as defined by Aubert & Droxler (1996). (*e*) Sea-level fluctuations during the last 5 Myr. Red arrows indicate systematic sea-level fall or regression during the Early Pleistocene and early Brunhes. Blue arrows mark intervals of clear sea-level rise and/or possible reflooding during Early Pleistocene super-interglacials and, in particular, the mid-Brunhes highest-amplitude observed transition in the Plio-Quaternary from glacial MIS 12 to interglacial MIS 11, which led to the initial bank-top reflooding at the origin of modern atolls. Data are from Miller et al. (2020). Abbreviations: kyr, thousand years; Ma, million years ago; MIS, marine isotope stage; MPWP, mid-Pliocene warm period; Myr, million years. Panels *a–d* adapted from Aubert & Droxler (1996).

during glacial MIS 16 and 12, equivalent to an LGM sea level at ∼125–135 m below sea level; Yokoyama et al. 2018 and references therein), became the substratum for reef development during the intervening intervals of sea-level rise, and the antecedent karst theory would therefore explain the stacked atoll development of the mid-to-late Brunhes (**Figure 11**).

If eustatic sea-level fluctuations were involved and played the most important forcing role in the formation of modern atolls, then this model should be observed globally, and not only in the atolls in the Maldives Archipelago.

4. MID-TO-LATE BRUNHES RIMS AND LAGOONS IN PACIFIC AND SOUTHWEST INDIAN OCEAN ATOLLS

Atoll rims and lagoon were drilled, particularly in the low latitudes of the Pacific, in the context of nuclear testing in the late 1940s, the 1950s, and the 1960s. It was on Bikini and Eniwetok Atolls (**Figure 1**) that basalt was initially encountered at the bottoms of two boreholes; at Eniwetok Atoll, the basalt was found 1.3 km below sea level, overlain by Eocene neritic dolomitic limestone and younger reefal limestone (Ladd et al. 1953), which for some proved Darwin's model. The published data from multiple boreholes drilled in Mururoa Atoll in French Polynesia (**Figure 1**) and one borehole drilled in Funafuti Atoll in Tuvalu (**Figure 1**) are integrated into this review. Other atolls have also been studied recently in the southwest Indian Ocean, where Pliocene drowned flat-topped banks have been reported in an active geodynamic context.

By revisiting some previous studies dedicated to modern atolls in the western Pacific and the southeastern Indian Ocean, we can ask some fundamental questions. Do the sedimentary and morphological patterns described for the Maldivian atolls also occur in other atolls, despite the differences in subsidence rates and overall settings? Is systematic development of late Pliocene flat-topped banks also observed? Are the Early Pleistocene and early Brunhes defined mostly by the presence of karsts and/or nondeposition? And how similar and comparable is the mid-to-late Brunhes stratigraphic expression of their rim building as five or more stacked coral-growth intervals separated by exposure horizons?

4.1. Mururoa Atoll

Mururoa Atoll, located in the south-central Pacific (21°50′S, 138°53′W) (**Figure 1**), belongs to the Tuamotu Archipelago in French Polynesia. This open atoll has an irregular elliptical shape and is

28 km long and 11 km wide, covering a total surface area of nearly 155 km^2 (**Figure 12*a***). In the southwest, the atoll rim surface is submerged, allowing the oceanic swell to directly enter the lagoon, which is 135 km^2 in surface area and has water depths of 28–52 m (Montaggioni et al. 2015).

Mururoa Atoll presents several advantages. Vertical and oblique boreholes have penetrated its coral-reef rim (Braithwaite & Camoin 2011, Camoin et al. 2001) as well as its lagoon (Buigues 1998), and some have drilled down to the top of volcanic edifice (Oligocene to Miocene in age, with a cessation of the volcanic activity at 11–10.5 Ma; Gillot et al. 1992), roughly providing a three-dimensional view of the buried volcanic top morphology (**Figure 12*b***). Several attempts at forward modeling using established sea-level records, subsidence rates, and other parameters have been published (Montaggioni et al. 2015) (**Figure 13*b***).

The estimated subsidence rates for Mururoa Atoll differ according to different authors, ranging from 30 m/Myr (Aïssaoui et al. 1990) to 70–80 m/Myr (Trichet et al. 1984). The stratigraphic modeling published by Montaggioni et al. (2015) (**Figure 13*b***) included an even greater subsidence rate of 105 m/Myr, combined with a stepwise increase of the carbonate production rates from 0.5 to 8 mm per year between 1.8 Ma and today, in order to successfully reproduce the geometry and the stratigraphic pattern observed by drilling (Braithwaite & Camoin 2011, Camoin et al. 2001).

Three major platforms were successively developed at Mururoa above the volcanic substratum (**Figure 12*c***). A relatively flat-topped late Miocene platform culminates at approximately 140 m below the modern lagoon seafloor, with a top marked by some subaerial exposure lines of evidence. Also affected by multiple exposures is a flat-topped late Pliocene platform that lies approximately 90 m below the modern lagoon seafloor. The late Pliocene platform apparently evolved into a possible atoll-like morphology when its margin developed a 10-m-high aggrading rim at the very end of the Pliocene, from 3.1 to 2.5 Ma (**Figure 12*c***). A major unconformity then occurs in the drilled sections of the lagoon and the rim, representing the Early Pleistocene and early Brunhes. The upper 80 m of the rim, directly overlying the late Pliocene rim, corresponds to stacked interglacials MIS 13/11 to MIS 1, separated by exposure horizons. Oblique drilling has allowed the recovery of stacked lowstand reefal deposits from glacial MIS 8 to MIS 2, onlapping the margin upper slope (**Figure 13*a***). The growth of the rim during the late Quaternary has been tested by forward stratigraphic modeling, which confirmed that most of the true framework of the Mururoa Atoll coral rim was not initiated prior to the mid-Brunhes (Montaggioni et al. 2015) (**Figure 13*b***). This increase in the reef aggradation of the atoll rim since the mid-Brunhes is also suggested by magnetostratigraphic dating along the Françoise well, which indicates a dramatic increase in reef accumulation rates (Aïssaoui et al. 1990) (**Figure 13*c***).

Our knowledge of sea-level fluctuations during the early to late Pliocene (Grant et al. 2019, Miller et al. 2020) suggests that sea-level stagnation (referred to as a stillstand) during the MPWP (the late Pliocene interval centered at 3.2 Ma and lasting at least 80 kyr; **Figure 4*c*,*d***) did not generate sufficient accommodation space for much vertical reef growth or aggradation. The extra neritic production would have been sufficient to fill in any existing lagoons through sand-apron progradations into the lagoon—as is currently occurring, for instance, in the Rasdhoo Atoll lagoon (**Figure 10*f***)—because the sea level has remained approximately constant since it reached the present level. This stillstand would therefore generate the observed late Pliocene flat-topped bank in Mururoa (**Figure 12*d***), similar to the multiple late Pliocene flat-topped banks observed in the Maldives. The brief sea-level fall at 3.15 Ma post-MPWP and a series of significant sea-level rises and falls of approximately 40 m in amplitudes until 2.6 Ma (**Figure 4*a*,*c***) would have favored the formation of a small, 10-m-thick rim during the latest Pliocene, as shown in **Figure 12*d***. As in its rim, a major unconformity occurs in the lagoon sequence, spanning the Early Pleistocene and the early Brunhes, a 2-Myr interval when sea level dropped in a stepwise fashion, tied to

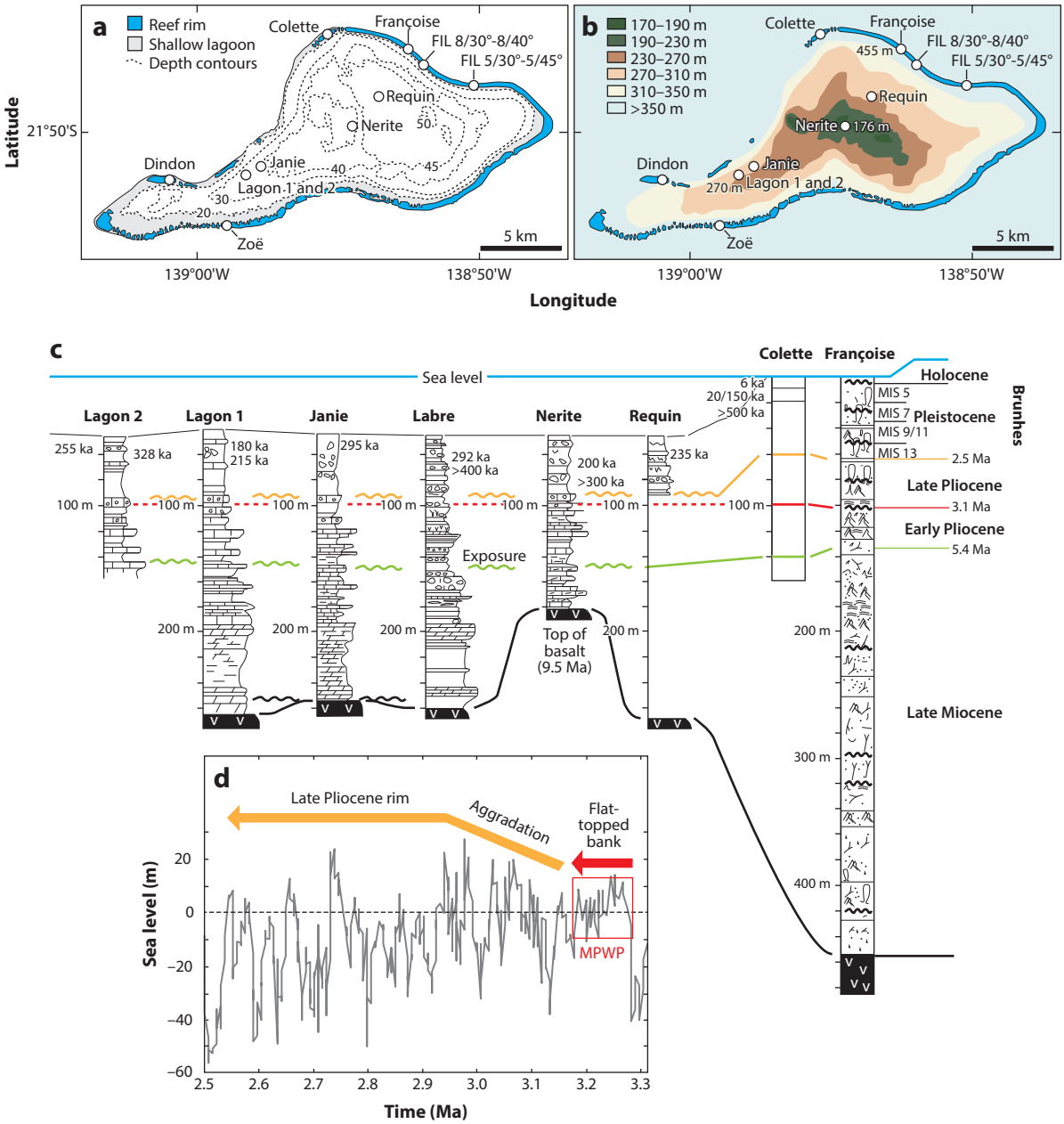

Figure 12

(*a*) Map illustrating the main bathymetric features of Mururoa Atoll (for location, see **Figure 1**), along with the locations of drill sites (*circles*) in its lagoon and coralgal rim. (*b*) Depth map of the volcanic edifice top basalt surface underlying the late Miocene to Holocene reef sequences. (*c*) Lithology and datings along wells drilled in the lagoon and on the rim of Mururoa Atoll. Note the major 2-Myr-long unconformity, representing exposure and karstification, in the lagoon and rim cores, where mid-Brunhes lagoonal and coral deposits, respectively, are overlain on late Pliocene neritic carbonates. MIS numbers for the Pleistocene unit in the Françoise well are from Braithwaite & Camoin (2011) and Camoin et al. (2001). (*d*) Sea-level changes during the early to late Pliocene (including the MPWP). Data are from Miller et al. (2020). Abbreviations: ka, thousand years ago; Ma, million years ago; Myr, million years; MIS, marine isotope stage; MPWP, mid-Pliocene warm period. Panel *a* adapted from Montaggioni et al. (2015); panel *b* adapted from Guille et al. (1993); panel *c* adapted from Buigues (1998).

the systematic increase of ice volume since the onset of the Northern Hemisphere glaciations at 2.5 Ma. The final aggradation of the rim in Mururoa since the mid-Brunhes confirms that deglacial and interglacial reefal growth intervals stacked successively above one another, each separated by typical horizons representing multiple long episodes of subaerial exposures, as reported on several

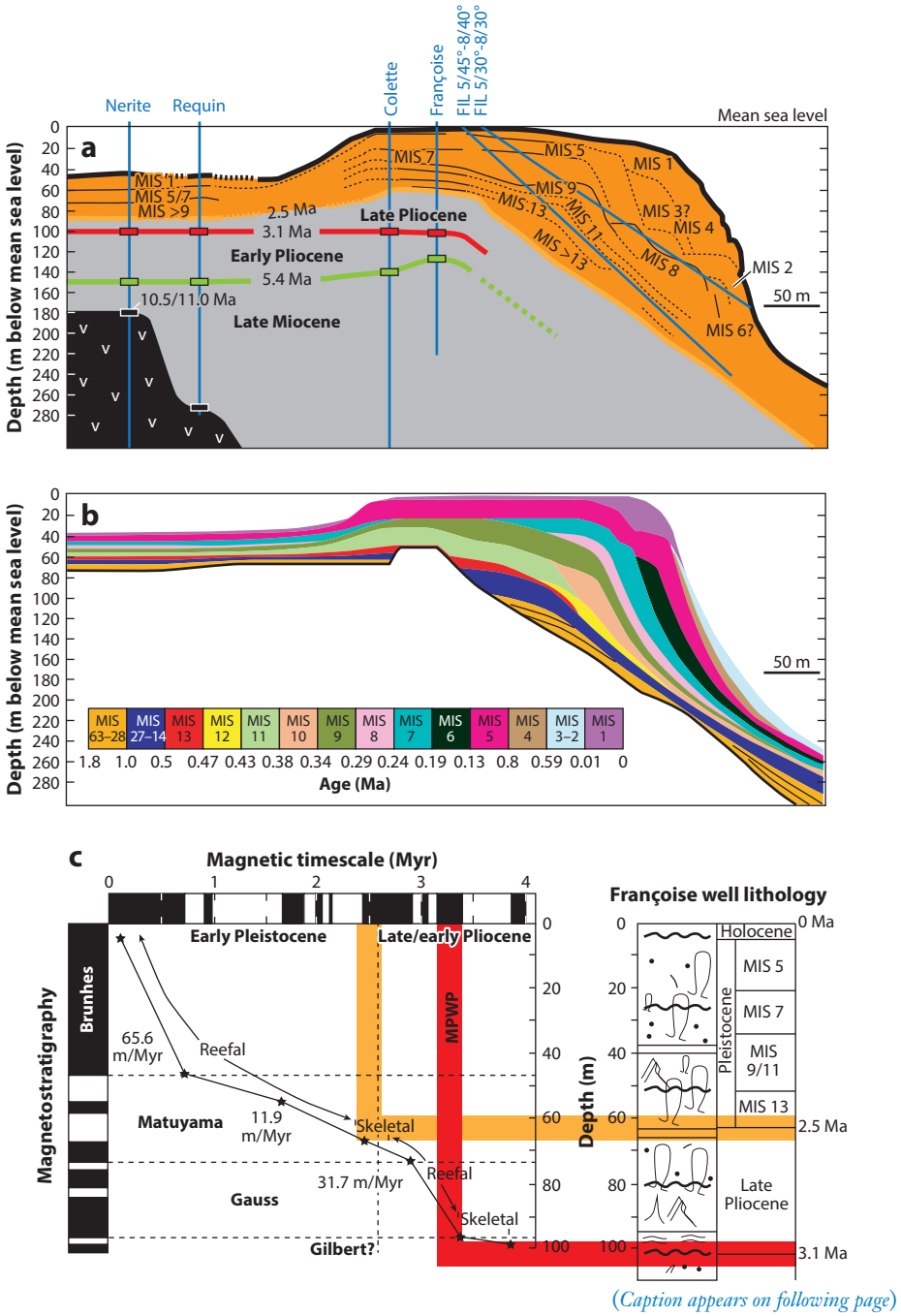

(*Caption appears on following page*)

Figure 13 (*Figure appears on preceding page*)

(*a*) The locations and alignments of both vertical and oblique drill holes along an idealized cross section through Mururoa Atoll, oriented west–southwest to east–northeast. This cross section well illustrates the vertical succession and stratigraphy of the mid-Brunhes carbonate section beneath the Mururoa Atoll modern outer rim and the lagoon, overlying the late Pliocene neritic carbonates, representing a 2-Myr-long unconformity due to exposure and karstification. The mid-Brunhes carbonate lagoon and rim sections consist of vertically stacked, mostly interglacial, accumulation during times of atoll reflooding, separated by exposure horizons; individual interglacial MIS intervals are identified based on the radiometric ages of coral samples extracted from the lagoon and rim cores. (*b*) Two-dimensional modeling of the last 1.8 Myr of the Quaternary carbonates deposited on Mururoa Atoll. Each color refers to a defined MIS time interval from MIS 63 to MIS 1. Note that the majority of the carbonate accumulation occurred in the lagoon and in particular along the rim since MIS 11, which well illustrates the middle and late Brunhes origin of the modern atoll. (*c*) Age/depth curve and lithology for the top 100-m in the Françoise vertical well, drilled on the rim of Mururoa Atoll. Note that the period of ∼50-m-thick coral-reef accumulation since the mid-Brunhes (MIS 11), overlying Late Pliocene carbonates, displays the highest rate of reef growth (65.6 m/Myr), and corresponds to the building of the modern Mururoa Atoll rim. Abbreviations: Ma, million years ago; MIS, marine isotope stage; MPWP, mid-Pliocene warm period; Myr, million years. Panel *a* adapted from Camoin et al. (2001), Ebren (1996), Montaggioni et al. (2015), and Perrin (1989); panel *b* adapted from Montaggioni et al. (2015); panel *c* adapted from Aïssaoui et al. (1990) and Buigues (1998).

Maldivian atolls for the last glacial cycles, such as Rasdhoo Atoll (Gischler et al. 2008) (**Figure 10*f***) and Maalhosmadulu Atoll (Kench et al. 2009).

4.2. Funafuti Atoll

Funafuti Atoll, located in the tropical South Pacific (8°30′S, 179°12′E) (**Figure 1**), is one atoll among many of the Tuvalu group (**Figure 14*a***). This atoll was drilled between 1896 and 1898 to test the subsidence theory developed by Darwin (1842). However, because the borehole did not penetrate the basement, it covers only the last 2 Myr, which makes this case study less useful than that of Mururoa Atoll. In addition, only one borehole was drilled, and the stratigraphic framework is constrained exclusively by ^{14}C- and strontium-isotope measurements, some of which might have issues because of dolomitization. On the other hand, the drilled ∼330-m-thick section, representing only the last 2 Myr, should reveal a high-resolution record of the atoll's evolution.

The top 110-m-thick rim of Funafuti Atoll is composed of several vertically stacked interglacial reefal units separated by distinct exposure horizons. The interglacial units were dated using strontium-isotope stratigraphy and were most likely from the mid-Brunhes (Ohde et al. 2002). Tentatively, the top 65 m was assigned to several stacked interglacials from MIS 11 or later, and the interval between 110 and 65 m was assigned to MIS 15 or 17; however, because of the large error bars, the latter interval could be younger, close to the mid-Brunhes in age (**Figure 14*b***). These successive interglacial reef growth units are separated by subaerial exposures. The intermediate reefal interval from 235 to 110 m, spanning in time from approximately 1.5 to 1.0 Ma, consists of two distinguished units separated by unconformities, which were interpreted to possibly coincide with the two strong interglacial intervals and strong highstands, MIS 47–45 and MIS 37–31 (Miller et al. 2020) (**Figure 14*c*,*d***). At the lower interval, from 330 m to 235 m, a dolomitized reef package yielded ages of approximately 2.0 Ma and could be interpreted to correspond to another strong interglacial and highstand interval, MIS 77–75 (**Figure 14*c***). Our above-mentioned interpretation is based on strontium-isotopes ages and therefore should to be considered with caution.

The subsidence rate in Funafuti has been estimated at 30 m/Myr (Ohde et al. 2002), which appears very slow when looking at the borehole record. The super-interglacial MIS 77–75 unit was dated to be ∼2 Myr old at a depth of ∼250 m, the MIS 49–47 unit was dated to be 1.45 Myr

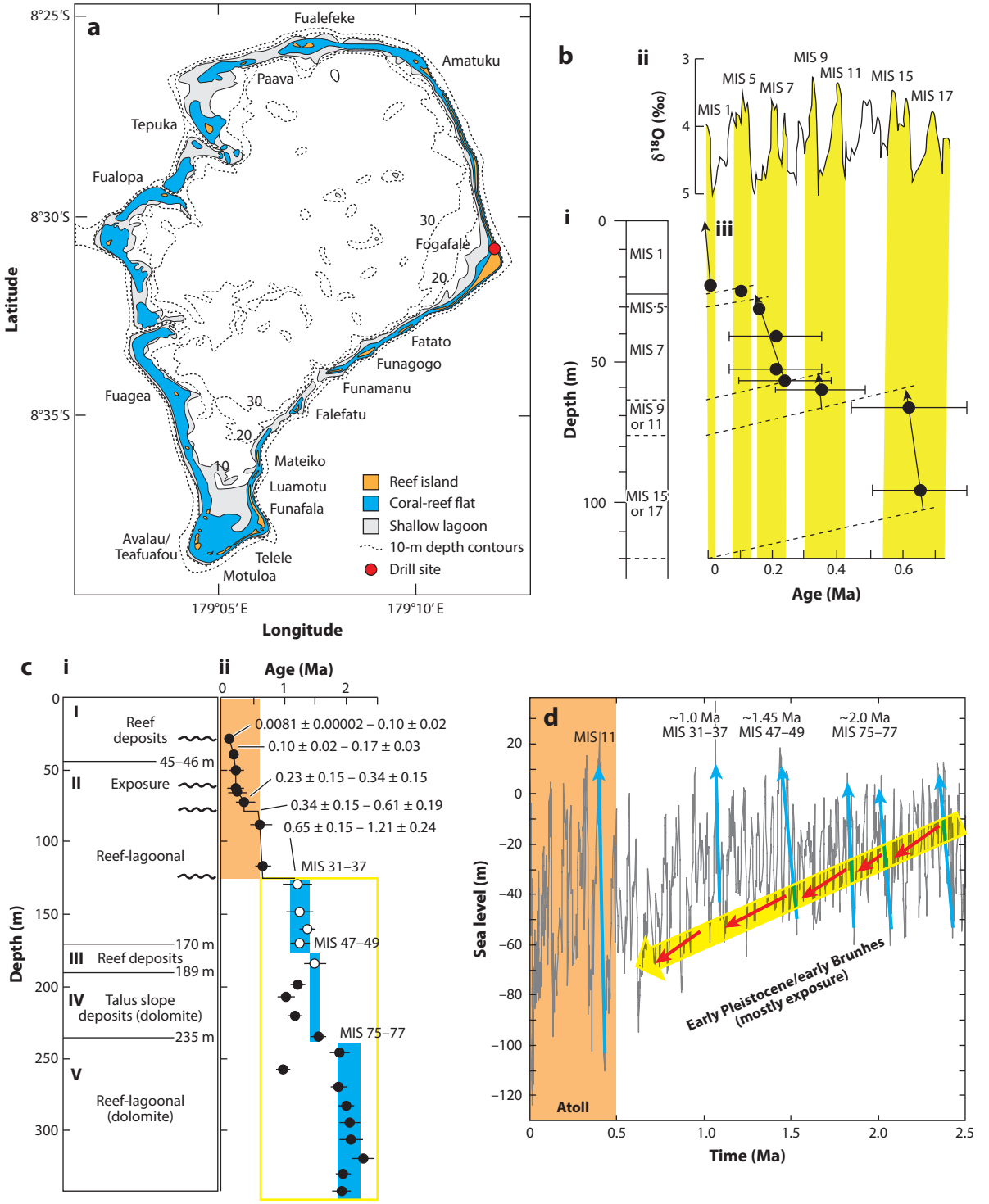

(Caption appears on following page)

Figure 14 (*Figure appears on preceding page*)

(*a*) Map of Funafuti Atoll (for location, see **Figure 1**), showing its lagoon bathymetry and rim coral-reef flat on which the drill site (*red circle*) is located. (*b*) The top 100 m of the borehole (subpanel *i*) corresponds to a series of five stacked reefal units separated by clear exposure karstic horizons, correlated with the ODP 677 (Shackleton et al. 1990) oxygen-isotope record (subpanel *ii*). Based on ages from strontium-isotope stratigraphy, with age uncertainties increasing with time, and their correlation with the oxygen-isotope record, each of these units corresponds to the atoll rim growth during the MIS 1–15 interglacials and inferred hiatuses between them, due to exposure and karstification during glacial sea level lowering. The top 100-m-thick coral-reef accumulation, therefore, is clearly middle to late Brunhes in age. The dashed lines in subpanel *ii* illustrate the uniform subsidence rate (30 m/Myr) in the age/depth model. (*c*, *i*) The top 330 m of the Funafuti borehole is divided into five lithologic units (Grimsdale 1952). (*ii*) Based on strontium-isotope age grouping, four main sedimentary packages are identified, separated by three major unconformities, often characterized by exposure and karstified horizons. The top 100–120 m corresponds to the middle to late Brunhes (see details in panel *b*). The ages of the package between 120 and 170 m apparently fall within super-interglacials MIS 31–37, between 170 and 235 m (excluding the age reversal, most likely related to dolomitization) within super-interglacials MIS 47–49, and between 235 and 330 m within super-interglacials MIS 75–77. (*d*) Sea-level fluctuations during the last 5 Myr from Miller et al. (2020). The four main reefal and neritic carbonate packages, defined based on strontium-isotope age grouping (see panel *c*, subpanel *ii*), correspond to major deglacial refloodings (*blue arrows*) initiating super-interglacial sea-level highstands similar to today's. Abbreviations: Ma, million years ago; MIS, marine isotope stage; Myr, million years; ODP, Ocean Drilling Program. Panel *a* adapted from Kench et al. (2015); panel *b* adapted from Ohde et al. (2002); panel *c* adapted from Grimsdale (1952) (subpanel *i*) and Ohde et al. (2002) (subpanel *ii*).

old at ~185 m, and the MIS 37–31 unit was dated to be 1.0 Myr old at ~125 m (**Figure 14*c***), yielding a rather constant average subsidence rate of ~125 m/Myr, according to our interpretation. Despite these different geodynamic settings, the evolution of Funafuti Atoll is very similar to what is observed in the Maldives and Mururoa Atoll. Data from Funafuti reflect the transition at the mid-Brunhes, marked by the end of the gradual deterioration of the climate from the Early Pleistocene to the early Brunhes at ~0.6–0.5 Ma (MIS 15–13), when the large error bars in the dating are taken into consideration. The mid-Brunhes transition is clearly marked by the occurrence of the exceptional high-amplitude deglacial sea-level rise, leading to the long and warm MIS 11 interglacial (Droxler et al. 2003 and references therein).

4.3. Bassas da India Atoll

The Mozambique Channel, located in the southwest Indian Ocean, is characterized by several modern carbonate platforms that range in latitude from 11°S to 21°S (Jorry et al. 2016). These platforms are characterized by reef margins developed mainly on windward sides, with lagoons blanketed by sand dunes and numerous reef pinnacles, or as Darwin-type atolls with enclosed lagoons, such as Bassas da India Atoll (**Figures 1** and **15*a***). Dredge sampling, underwater observations, and geophysical acquisitions carried out during recent oceanographic cruises (Jorry 2014, Jouet & Deville 2015) led to the discovery of flat-topped terraces along the southern slope of Bassas da India, corresponding to shallow-water carbonate platforms that grew on top of a submarine volcano (Courgeon et al. 2016, 2017) (**Figure 15*b***). The volcanism in this region has been dated to have occurred from the late Oligocene to early Miocene (Courgeon et al. 2016). Microfacies analysis and dating of the drowned platforms (biostratigraphy analysis coupled with strontium-isotope stratigraphy) indicate that those platforms—which are characterized by fauna assemblages dominated by corals, green algae such as *Halimeda*, red algae, and larger benthic foraminifera—developed in tropical settings from the late Miocene to late Pliocene (Courgeon et al. 2016). Evidence of submarine volcanism, karstification, and pedogenesis on top of the drowned edifices demonstrates that tectonic deformation, rejuvenated volcanic activity, and subaerial exposure occurred after and potentially during the Neogene platform aggradation (Courgeon et al. 2017). The growth of the modern atoll on top of submerged carbonate terraces is explained by topographic irregularities inherited from volcanism, tectonic, and/or subaerial

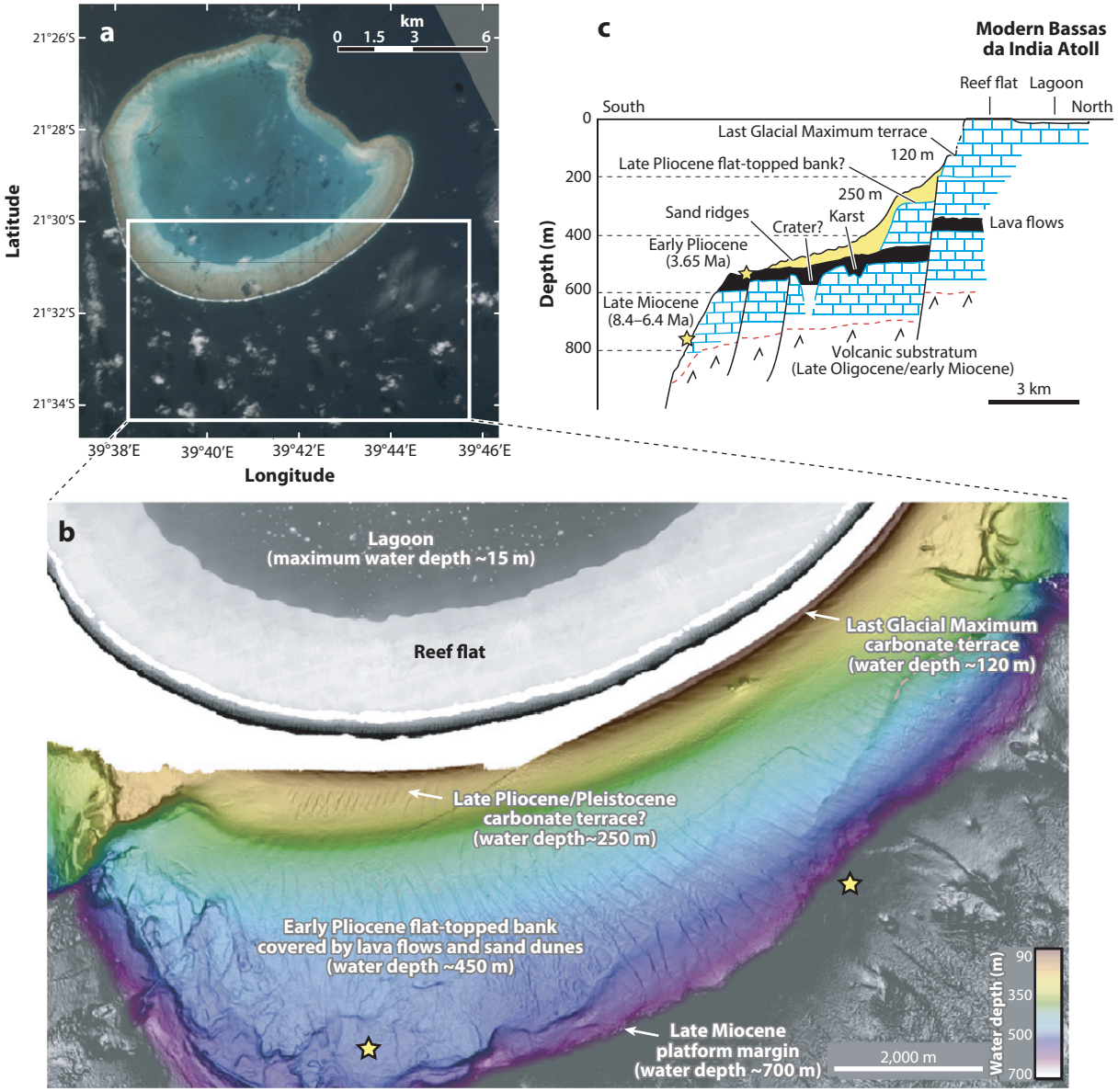

Figure 15

(*a*) Google Earth satellite image of Bassas da India Atoll, located in the Mozambique Channel (for location, see **Figure 1**). (*b*) Lidar bathymetry of Bassas da India Atoll with a rim fully flooded during high tides, along with high-resolution multibeam-based bathymetry at 10-m contour intervals. (*c*) Schematic cross section of Bassas da India Atoll, illustrating the topographic evolution of the platform since the late Miocene. In panels *b* and *c*, several submerged carbonate terraces are clearly visible on the southeastern upper slopes of the modern atoll (Courgeon et al. 2016), including a late Miocene platform margin, an early Pliocene flat-topped bank (presently covered by deep-water sand dunes, as detailed in Miramontes et al. 2019), a late Pliocene/Pleistocene flat-topped terrace, and a Last Glacial Maximum terrace lying at a water depth of approximately 120 m. Late Oligocene/early Miocene volcanism created the main substratum for the late Miocene platform, which was subsequently intruded upon by rejuvenated volcanism during the early Pliocene, with lava flows covering its top. The terrace, illustrating a flat-topped bank in the late Pliocene (currently at 250 m below sea level), served as a favorable substrate for the growth of the atoll since the mid-Brunhes. Yellow stars indicate the locations of dredges analyzed by Courgeon et al. (2017). Faults have been inferred from both bathymetry and seismic data (see Courgeon et al. 2017). Abbreviation: Ma, million years ago. Panel *c* adapted from Courgeon et al. (2017).

exposure conditions that could have produced a favorable substratum for carbonates during the Plio-Quaternary, up to modern sea levels (Courgeon et al. 2017). Despite a strong impact of tectonics on the evolution of these successive platforms, which is related to the geodynamic activity of the East African Rift system (Courgeon et al. 2018, Deville et al. 2018), flat-topped banks developed during the Quaternary, before the formation of the modern Bassas da India Atoll (**Figure 15*c***). Interestingly, considering a fault offset of approximately 50 m, the late Miocene and late Pliocene drowned terraces (which are located at water depths of 450 m and 250 m, respectively; **Figure 15*c***) might be analogous to the drowned carbonate banks in the Maldives (which are located at water depths of approximately 600 m and 230 m).

5. DISCUSSION AND CONCLUSIONS

The Maldives is unique in terms of its numerous atolls, their size range, and their organization. The atolls represent only a tiny fraction of the extensive 2–3-km-thick submerged Maldivian carbonate megaplatform. This megaplatform is rooted in a volcanic plateau formed as part of the hot-spot trail of the island of Réunion; this plateau was once exposed on land and then subsided slowly enough for the neritic carbonates to fill the accommodation space and remain within the photic zone, explaining its 2–3-km thickness (**Figures 7** and **16**).

The 55-Myr growth of the Maldivian megaplatform is complex, and the well-developed atolls that characterize its modern expression correspond only to the final phase of its evolution (**Figure 7*b***). The volcanic plateau influenced only the size and the morphology of the carbonate megaplatform until the very end of the Oligocene, when the platform almost fully drowned (P1/P2 in **Figure 16**). In losing the connection with their volcanic roots, two separated, continuous, elongated platforms survived and recovered through aggradation and some progradation on the eastern and western margins of the Oligocene carbonate system during the early part of the Neogene (N1/N2 in **Figure 16**). Both platforms enclosed a deep basin between them, today referred to as the Inner Sea. Slightly earlier than the middle to late Miocene boundary, at approximately 13 Ma, when the sea level was falling and the monsoon abruptly began (Betzler et al. 2016b), both platforms were partially drowned and became segmented, separated by channels connecting the Inner Sea with the open ocean (Aubert & Droxler 1992, 1996; Belopolsky & Droxler 2003, 2004; Lüdmann et al. 2013, 2018) (N3 in **Figure 16**). Strong currents flowed through these channels, and at their mouths, extensive and thick prograding sediment piles accumulated and prograded along the platform's upper slope (Aubert & Droxler 1992, 1996; Belopolsky & Droxler 2003, 2004), which IODP Expedition 359 interpreted as carbonate delta drifts (Lüdmann et al. 2018). In the central part of the Maldives, in the area of the Kardiva Channel, the platforms mostly aggraded during the late Miocene and Pliocene while their segmentation continued, and they became well-developed flat-topped banks at approximately 235–250 m of water depth (N4/N5 in **Figure 16**). Some of these Pliocene flat-topped banks, as in the northern part of Ari Atoll and the southeastern part of Ghoidoo Atoll, partially drowned at the end of the Pliocene, while at the same time, the platform between them, today known as Fuad Bank, fully drowned and is still exposed at the seafloor in 235 m of water depth (**Figure 16**). The modern Ari and Goidhoo platforms continued to aggrade mostly vertically and ultimately transformed into the atolls we know today (**Figure 16**).

The common roots of the mid-to-late Brunhes atolls in the Maldives, Mururoa Atoll, and Bassas da India Atoll are late Pliocene flat-topped banks. In the case of Funafuti Atoll, the borehole was not deep enough to reach the late Pliocene. The drilling ended approximately 330 m below sea level in a reefal deposit dated as 2 Myr old, short of reaching the late Pliocene flat-topped banks (approximately 3.1–3.3 Myr old) observed in the Maldives and in Bassas da India Atoll, and located

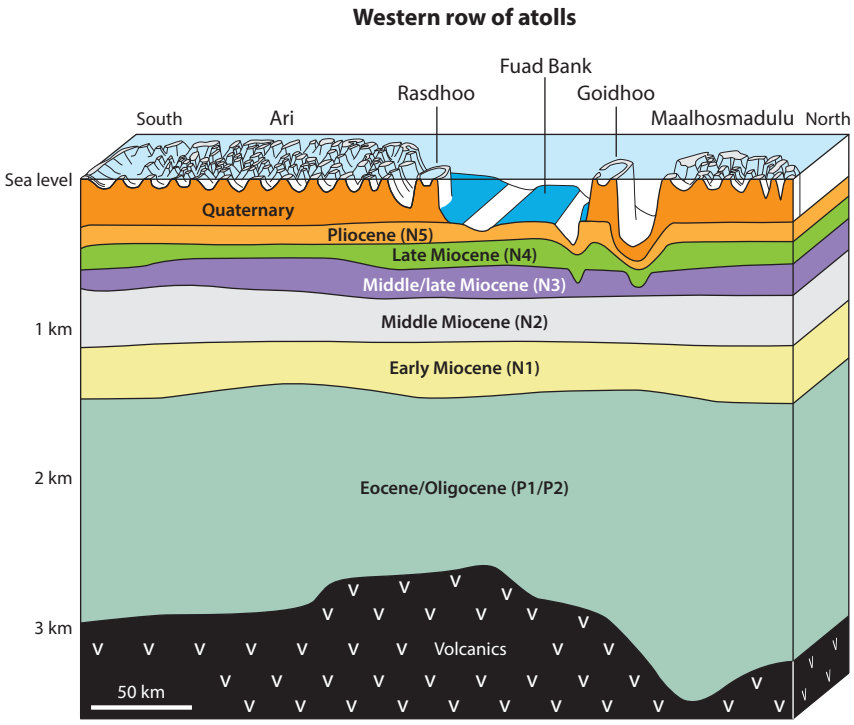

Figure 16

Three-dimensional representation of a north–south depth-converted transect across the Maldivian western atoll chain, from Ari Atoll to South Maalhosmadulu Atoll (for location, see **Figure 6**). The megaplatform was established and grew in the middle and late Paleogene (P1/P2) influenced by the morphology of the underlying volcanic plateau. The megaplatform was almost fully drowned at the end of the Oligocene and only grew by aggradation as continuous elongated platforms on both its margins during the early Neogene (N1/N2). The initial segmentation of these platforms occurred at the middle/late Miocene boundary (N3) between Goidhoo Atoll and the northern part of Fuad Bank. Their segmentation and aggradation continued during the late Miocene and Pliocene (N4/N5) between the southern part of Fuad Bank and the northern part of Ari Atoll. The late Pliocene flat-topped banks became either fully drowned (Fuad Bank) or partially drowned (North Ari Atoll and southeastern Goidhoo Atoll), where the other parts of the segmented late Pliocene platforms evolved during the late Quaternary, in particular since the middle and late Brunhes, into the modern atoll we know today. Figure adapted from Aubert & Droxler (1996).

at approximately 230–250 m below sea level, whereas the late Pliocene flat-topped bank under Mururoa Atoll was drilled at approximately 100 m below sea level. These observations clearly indicate that the subsidence rates of the four atoll examples included in this review range from high for the Funafuti Atoll (330 m in 2 Myr, or ~165 m/Myr) to low for Mururoa Atoll (100 m in 3.1 Myr, or ~32 m/Myr), while the Maldivian atolls and Bassas da India Atoll had average rates (230–250 m in 3.1 Myr, or ~80 m/Myr). The subsidence rates calculated in the Maldives based on the current water depths of the late Pliocene flat-topped bank—approximately 80 m/Myr—correspond well with low end members of the subsidence rate range, 50–90 m/Myr (as calculated in Gischler et al. 2018), using the top of the MIS 5e reefs encountered in one of the boreholes drilled on the margin of Rasdhoo Atoll.

In contrast to the observed subsidence rate ranges, the rates of sea-level fluctuation since the Pliocene can be as great as meters per century, as observed during some of the major meltwater

pulses during the last deglaciation (Abdul et al. 2016, Deschamps et al. 2012) and the acute ice-sheet growth interval during the Last Glacial Maximum (Yokoyama et al. 2018). The rates of sea-level rise in the late Quaternary, when averaged for the last full deglacial 130-m amplitude of rise in approximately 14 kyr, are as high as 9 m/kyr (9,000 m/Myr), which is two orders of magnitude greater than the 80-m/Myr subsidence rate estimated for the Maldives. Rates of sea-level fall during the last glacial cycle—for instance, at the transitions between MIS 5e and 5d and between MIS 3 and 2—are very similar to those during the last deglaciation. Finally, the rates of sea-level rise and fall for the mid-to-late Brunhes are obviously overwhelmingly greater than the subsidence rates of the carbonate platforms and their underlying volcanic edifices included in this review. However, the combination of sea level falling and rising in the context of such a wide range of atoll subsidence rates should yield different sedimentary responses:

- In the early Pliocene, sea level remained unusually constant, as in part of the late Pliocene during the MPWP (Miller et al. 2020) (**Figure 17*f***). If atolls formed during the Pliocene, their lagoons would be filled and the atolls would evolve into flat-topped banks (**Figure 17*a***), which might also expand laterally through progradation.
- At the end of the Pliocene, sea level briefly fell before rising quite significantly, forming a possible atoll in Mururoa (**Figures 12**, **13**, and **17*b*,*f***), whereas some of the late Pliocene flat-topped banks in the Maldives drowned or partially drowned and others continued to aggrade (**Figure 16** and **17*b***).
- Since the onset of major glaciations in the Northern Hemisphere, global ice volume increased systematically from the Early Pleistocene to the early Brunhes to reach a first maxima of ice volume at the MIS 16 and MIS 12 glacial intervals, roughly equivalent to the well-constrained low sea level for the Last Glacial Maximum (MIS 2), at approximately 125–135 m below the present sea level (Spratt & Lisiecki 2016 and references therein). The systematic ice-volume growth during this 2-Myr period translated overall into a dramatic stepwise sea-level fall that was interrupted by four intervals of super-interglacial deglaciations at approximately 2.4, 2.0, 1.5, and 1.0 Ma (**Figure 17*e***). Mururoa Atoll has a major unconformity under its lagoon and rim that formed through a combination of no deposition and karstification, the sea level being too low to even intermittently reflood the late Pliocene flat-topped banks that were being karstified (**Figures 12** and **13**). In the Maldives, the systematic lowering of sea level or the downward shift of base level is clearly recorded in a series of downward shifts in the accumulation of sedimentary wedges onlapping the upper slopes of the late Pliocene flat-topped bank, which were mostly exposed and karstified during this particular interval, with possibly temporary reflooding during four super-interglacial deglaciations at approximately 2.4, 2.0, 1.5, and 1.0 Ma (**Figure 11**). In Funafuti Atoll, because of its fast subsidence rates, the relative sea-level fall amplitude would have been minimized, and sea level periodically reflooded the exposed and karstified Pliocene flat-topped bank during each of the superglacial intervals at 2.0, 1.5, and 1.0 Ma, as shown in the Funafuti borehole record (**Figure 14*c***).
- Since the mid-Brunhes, high-amplitude cyclic sea-level changes of 125–135 m approximately every 100 kyr mostly kept the bank tops exposed and subjected them to karstification for 80% of the time, while stacked reef growth at their margins occurred when the banks were reflooded during peak interglacials, such as MIS 11, 9, 7, 5, and 1 (**Figure 17*d*,*e***).

Moreover, the Plio-Quaternary atoll evolution in the Maldives and in the west Pacific Ocean and southwest tropical Indian Ocean bears interesting similarities to the evolution of mixed carbonate/siliciclastic continental shelves, such as the shelf in the Gulf of Papua (figure 13 in Droxler & Jorry 2013). During the Pliocene, in the southwestern corner of the Gulf of Papua,

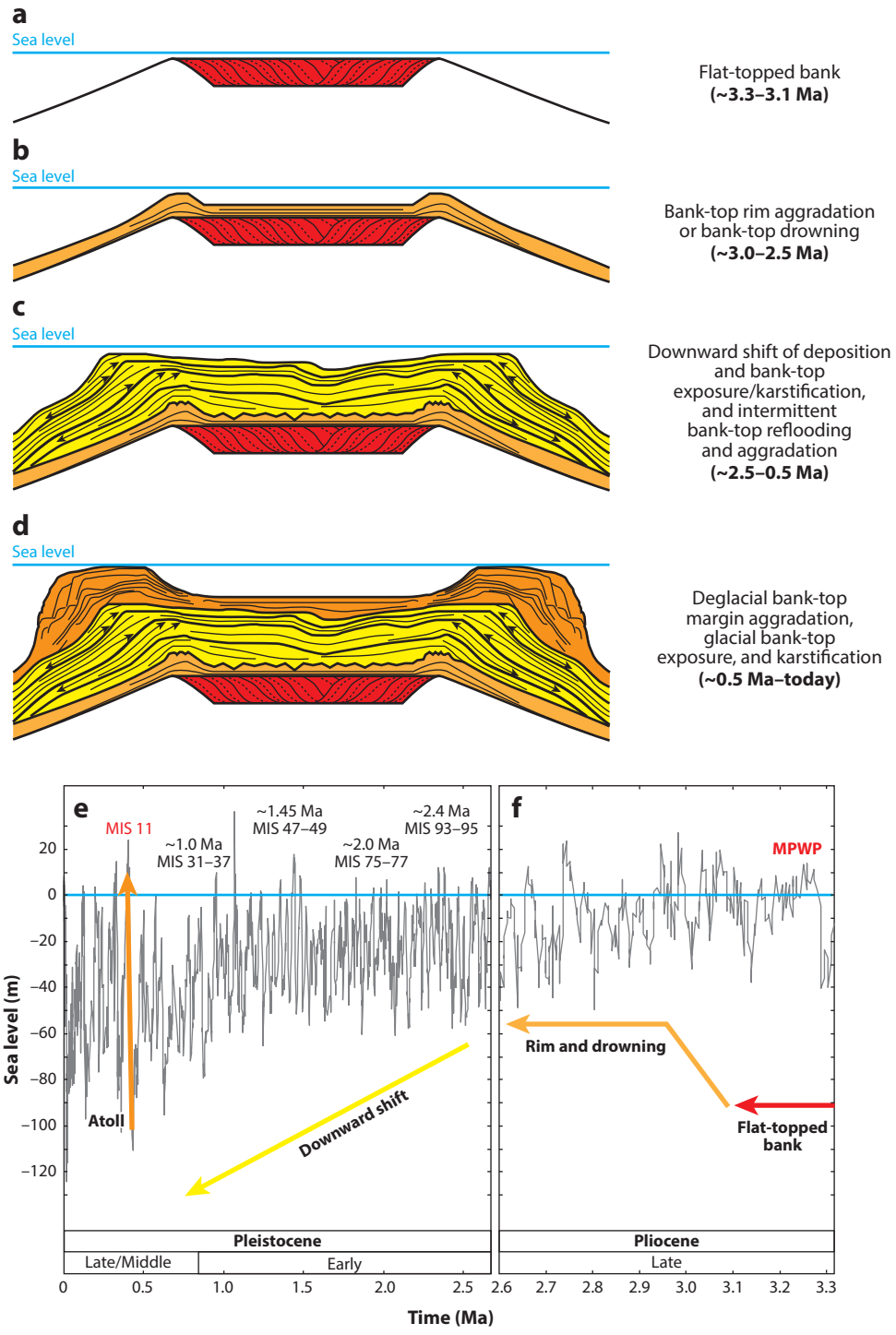

(*Caption appears on following page*)

Figure 17 (*Figure appears on preceding page*)

Improved antecedent karst model to explain the origin of modern atolls, based on our current knowledge of well-established Plio-Quaternary sea-level fluctuations with no direct involvement of their volcanic substratum, as a more realistic alternative to the Darwin volcanic edifice subsidence model. (*a*) Development of a late Pliocene flat-topped bank during the MPWP, when any existing lagoons would have been filled as a response to an 80-kyr interval when sea level remained unusually constant. (*b*) At the end of the Pliocene, some coral rims grew vertically on the edges of the flat-topped banks, trying to keep up with the rates of sea-level rise (e.g., Mururoa Atoll), while some other platforms fully drowned (e.g., Fuad Bank), partly drowned (e.g., the northern part of Ari Atoll and the southeastern part of Goidhoo Atoll), or continued to vertically aggrade (e.g., many atolls in the Maldives). (*c*) The systematic lowering of sea level or the downward shift of base level during the Early Pleistocene–early Brunhes is characterized by the accumulation of stacked sedimentary wedges onlapping the upper slopes of the late Pliocene flat-topped bank, which were mostly exposed and karstified during this interval, with possibly temporary reflooding during four super-interglacial deglaciations at approximately 2.4, 2.0, 1.5, and 1.0 Ma. (*d*) Since the mid-Brunhes, stacked reef growth intervals separated by exposure horizons at the raised margins of karstified platforms occurred when the banks, after being exposed during glacial times, were reflooded during deglaciations and peak interglacials, such as MIS 11, 9, 7, 5, and 1. (*e*,*f*) The four different phases of modern atoll evolution (panels *a*–*d*) placed into the context of the Quaternary (panel *e*) and Late Pliocene (panel *f*) sea-level fluctuations (Miller et al. 2020). Abbreviations: Ma, million years ago; MIS, marine isotope stage; MPWP, mid-Pliocene warm period.

close to the present northern extremity of the modern Great Barrier Reef, a high-resolution seismic line, oriented perpendicular to the modern shelf edge (dip line), clearly shows a series of Pliocene deglacial and highstand aggrading and prograding reefs established on top of shelf-edge siliciclastic lowstand deltas and culminating, in the late Pliocene, in well-developed flat-topped banks. The Early Pleistocene is initially defined by a clear downward shift in deposition and then consists of a series of downstepping, prograding siliciclastic sequences, recording several forced regressions that were linked to the systematic global increase in ice volume (Miller et al. 2020) (**Figure 4*a***). Each siliciclastic sequence is bounded by high-amplitude reflections corresponding to carbonate-rich intervals associated with some small mound-like reef features on an updip position, stacked on top of the late Pliocene flat-topped banks. Therefore, these are interpreted as systematic reflooding events during the high-amplitude super-interglacial deglaciations at MIS 49–47 (~1.45 Ma), MIS 37–31 (~1.0 Ma), and MIS 11 (0.4 Ma). The most recent deglaciation following the Last Glacial Maximum corresponds to the high-amplitude reflections observed on today's outer shelf and the relict drowned shelf-edge transgressive barrier reef on the shelf edge itself.

In conclusion, the origin of modern late Quaternary atolls is independent of any influence of the volcanic basement. Modern atolls, therefore, did not originate in initial fringing reefs attached to a slowly subsiding volcanic edifice, evolve into barrier reefs, and then become atolls when the volcanic edifice was fully buried by its carbonate cap, as the Darwin subsidence model suggests. On the contrary, the late Quaternary atolls were initiated on late Pliocene flat-topped banks that formed during the MPWP, a warm and climatically stable 80-kyr time interval during which sea level did not fluctuate. Some of these flat-topped banks drowned or partially drowned during the sea-level rise at the end of the Pliocene, while others continued to grow into atolls.

The exposure of bank tops occurred during the 2-Myr (Early Pleistocene to early Brunhes) interval of ice-volume stepwise increase, creating a karstified bank-top morphology. The bank tops were flooded intermittently during some of the four super-interglacial intervals. The modern atolls originated in the mid-Brunhes, using the antecedent karst morphologies that formed during the previous 2 Myr. High-amplitude 125–135-m sea-level cycles at a 100-kyr eccentricity beat flooded the bank tops approximately five times, for about 20% of the full cycle, when coral reefs reestablished themselves (particularly along the bank margins), but not for long enough to fill the

atoll lagoons. During the late Quaternary (middle and late Brunhes), these successive short-term bank-top refloodings, following a succession of relatively longer exposure times that stimulated preferential erosion through karst dissolution in the center part of the exposed bank top, triggered coral growth preferentially along the raised bank margins and, therefore, enhanced the relief between reef margins and lagoon seafloors and created the templates for the modern atolls as we know them.

DISCLOSURE STATEMENT

The authors are not aware of any affiliations, memberships, funding, or financial holdings that might be perceived as affecting the objectivity of this review.

ACKNOWLEDGMENTS

This review has benefited from years of research on the evolution of carbonate systems at different timescales and in different parts of the world by A.W.D.'s research group at Rice University's Department of Earth, Environmental, and Planetary Sciences and by S.J.J.'s research group at IFREMER's Marine Geosciences Unit. Seismic data and interpretations illustrated in this article are from Rice University PhD dissertations and publications of Drs. Olivier Aubert and Andrei Belopolsky of Rice University. The financial, scientific, and technical support for research in the Maldives came initially from Elf Aquitaine (now Total); A.W.D. addresses a very special thanks to Drs. R. Jouhannnel and Philippe Lapointe of Total. Support was later provided by Royal Dutch Shell; our gratitude goes to Drs. Peter Suessli and M. Vannier, who provided seismic and well data. National Science Foundation grants partially funded A.W.D.'s research group.

Co–principal investigators Professors Jan Bachmann and Bob Duncan and the shipboard scientific party, officers, and crew of ODP Leg 115 are acknowledged for their support. We are grateful for the work and dedication of the scientists, officers, and crew members during 2009 R/V *Meteor* cruise M74/4, NEOMA (Neogene of the Maldives), led by chief scientist Professor Christian Betzler of the Institut für Geologie, Universität Hamburg. Special thanks to Ahmad Naseem, Dr. Shiham Adam, Dr. Ibrahim Mohamed, and Dr. Abdulla Naseer for their invaluable support in Malé, and to the National Science Foundation for a grant (0729070) awarded to A.W.D.

The multibeam data sets presented in this article were acquired by co–principal investigators A.W.D. and David F. Naar, with extensive field and data-processing support from Brian Donahue of the University of South Florida, St. Petersburg, and Dr. Pankaj Khanna, a former PhD student at Rice University. The different research programs in the Maldives through the years would not have happened without the personnel from the Environmental Research Center [now the Environmental Protection Agency (EPA) of the Republic of Maldives]. Special thanks go to Gordon Ewers and Aishath Farhath Ali for their logistic assistance and to Hussain Ibrahim for his assistance at sea with the captain and crew from the EPA. Multibeam funding was provided by the EPA and the University of South Florida. Data and interpretation from Bassas da India Atoll come from the PhD thesis of Dr. Simon Courgeon (Aix-Marseille University), funded by the PAMELA (Passive Margins Exploration Laboratories) research program led by IFREMER, Total, CNRS (Centre National de la Recherche Scientifique), the University of Rennes, the University of Western Brittany, UPMC (Université Pierre et Marie Curie), and IFPEN (IFP Energies Nouvelles). The shipboard scientific party, officers, and crew of the cruises PTOLEMEE (S.J.J., principal investigator) and PAMELA-MOZ4 (Dr. Gwenael Jouet and Dr. Eric Deville, principal investigators) are also acknowledged. Sylvain Bermell-Fleury (IFREMER) is warmly thanked for his contribution on the ETOPO1 Global Relief Model.

A.W.D., on the eve of his 33 years as a professor at Rice University, would like to recognize and acknowledge here his advisers, mentors, and colleagues, who have so strongly influenced his 40-year professional career as a marine geologist–oceanographer: Professor Jean-Paul Schaer at the University of Neuchâtel (Switzerland), Professors Wolfgang Schlager and Cesare Emiliani at the University of Miami's Rosenstiel School of Marine and Atmospheric Sciences (Florida) and Free University in Amsterdam (Netherlands), Dr. Carlos Cramez at Total in Paris (France), and Professors Albert Bally and Peter Vail at Rice University (Texas).

Finally, we warmly acknowledge Production Editor Jim Duncan for his thorough review and advice, Illustration Editor Glenda Mahoney for substantially improving the figures, Dr. Paul M. (Mitch) Harris for his review of an early version of the article, and Dr. Charles A. Nittrouer for helpful comments.

LITERATURE CITED

Abdul NA, Mortlock RA, Wright JD, Fairbanks RG. 2016. Younger Dryas sea level and meltwater pulse 1B recorded in Barbados reef crest coral *Acropora palmata*. *Paleoceanography* 31:330–44

Agassiz A. 1902. An expedition to the Maldives. *Am. J. Sci.* 13:297–308

Aïssaoui DM, McNeil DF, Kirschvink JL. 1990. Magnetostratigraphic dating of shallow-water carbonates from Mururoa atoll, French Polynesia: implications for global eustasy. *Earth Planet. Sci. Lett.* 97:102–12

Amante C, Eakins BW. 2009. *ETOPO1 1 Arc-Minute Global Relief Model: procedures, data sources and analysis*. Tech. Memo NESDIS NGDC-24, Natl. Geophys. Data Cent., Natl. Ocean. Atmos. Adm., Boulder, CO. **https://doi.org/10.7289/V5C8276M**

Aubert O, Droxler AW. 1992. General Cenozoic evolution of the Maldives carbonate system (equatorial Indian Ocean). *Bull. Cent. Rech. Explor.-Prod. Elf-Aquitaine* 16:113–36

Aubert O, Droxler AW. 1996. Seismic stratigraphy and depositional signatures of the Maldive carbonate system (Indian Ocean). *Mar. Pet. Geol.* 13:503–36

Backman J, Duncan RA. 1988a. Site 714. In *Proceedings of the Ocean Drilling Program, Initial Reports*, Vol. 115, pp. 847–915. College Station, TX: Ocean Drill. Program

Backman J, Duncan RA. 1988b. Site 716. In *Proceedings of the Ocean Drilling Program, Initial Reports*, Vol. 115, pp. 1005–73. College Station, TX: Ocean Drill. Program

Barrett SJ, Webster JM. 2012. Holocene evolution of the Great Barrier Reef: insights from 3D numerical modelling. *Sediment. Geol.* 265–66:56–57

Belopolsky AV, Droxler AW. 2003. Imaging Tertiary carbonate system—the Maldives, Indian Ocean: insights into carbonate sequence interpretation. *Lead. Edge* 22:646–52

Belopolsky AV, Droxler AW. 2004. Seismic expressions of prograding carbonate bank margins: Middle Miocene, Maldives, Indian Ocean. *AAPG Mem.* 81:267–90

Betzler C, Eberli GP, Alvarez Zarikian CA, Alonso-García M, Bialik OM, et al. 2017. Expedition 359 summary. In *Maldives Monsoon and Sea Level*, MS 359-101. Proc. Int. Ocean Discov. Program Vol. 359. College Station, TX: Int. Ocean Discov. Program

Betzler C, Eberli GP, Alvarez Zarikian CA, Exped. 359 Sci. 2016a. *Expedition 359 Preliminary Report: Maldives Monsoon and Sea Level*. College Station, TX: Int. Ocean Discov. Program

Betzler C, Eberli GP, Kroon D, Wright JD, Swart PK, et al. 2016b. The abrupt onset of the modern South Asian Monsoon winds. *Sci. Rep.* 6:29838

Betzler C, Hübscher C, Lindhorst S, Reijmer JJG, Römer M, et al. 2009. Monsoon-induced partial carbonate platform drowning (Maldives, Indian Ocean). *Geology* 37:867–70

Bonney TG. 1904. *The Atoll of Funafuti: Borings into a Coral Reef and the Results, Being the Report of the Coral Reef Committee of the Royal Society*. London: R. Soc. Lond.

Braithwaite CJR, Camoin GF. 2011. Diagenesis and sea-level change: lessons from Moruroa, French Polynesia. *Sedimentology* 58:259–84

Buigues DC. 1998. La couverture carbonatée d'un atoll: exemple de Mururoa et Fangataufa. *Géol. France* 3:87–96

Camoin GF, Ebren P, Eisenhauer A, Bard E, Faure G. 2001. A 300,000-yr coral reef record of sea level changes, Mururoa atoll (Tuamotu archipelago, French Polynesia). *Palaeogeogr. Palaeoclimatol. Palaeoecol.* 175:325–41

Courgeon S, Bachèlery P, Jouet G, Jorry SJ, Bou E, et al. 2018. The offshore east African rift system: new insights from the Sakalaves seamounts (Davie Ridge, SW Indian Ocean). *Terra Nova* 30:380–88

Courgeon S, Jorry SJ, Camoin GF, BouDagher-Fadel MK, Jouet G, et al. 2016. Growth and demise of Cenozoic isolated carbonate platforms: new insights from the Mozambique Channel seamounts (SW Indian Ocean). *Mar. Geol.* 380:90–105

Courgeon S, Jorry SJ, Jouet G, Camoin G, BouDagher-Fadel MK, et al. 2017. Impact of tectonic and volcanism on the Neogene evolution of isolated carbonate platforms (SW Indian Ocean). *Sediment. Geol.* 355:114–31

Daly R. 1915. The glacial-control theory of coral reefs. *Proc. Am. Acad. Arts Sci.* 51:155–251

Dana JD. 1872. *Corals and Coral Islands*. London: Sampson Low, Marston, Low and Searle

Darwin C. 1842. *The Structure and Distribution of Coral Reefs*. London: Smith, Elder and Co.

Davies PJ. 2011. Antecedent platforms. In *Encyclopedia of Modern Coral Reefs: Structure, Form and Process*, ed. D Hopley, pp. 40–47. Dordrecht, Neth.: Springer

Davis WM. 1928. *The Coral Reef Problem*. New York: Am. Geogr. Soc.

Deschamps P, Durand N, Bard E, Hamelin B, Camoin G, et al. 2012. Ice-sheet collapse and sea-level rise at the Bølling warming 14,600 years ago. *Nature* 483:559–64

Deville E, Marsset T, Courgeon S, Jatiault R, Ponte J-P, et al. 2018. Active fault system across the oceanic lithosphere of the Mozambique Channel: implications for the Nubia-Somalia southern plate boundary. *Earth Planet. Sci. Lett.* 502:210–20

Draut AE, Raymo ME, McManus JF, Oppo DW. 2003. Climate stability during the Pliocene warm period. *Paleoceanography* 18:1078

Droxler AW, Jorry SJ. 2013. Deglacial origin of barrier reefs along low-latitude mixed siliciclastic and carbonate continental shelf edges. *Annu. Rev. Mar. Sci.* 5:165–90

Droxler AW, Poore RZ, Burckle LH, eds. 2003. *Earth's Climate and Orbital Eccentricity: The Marine Isotope Stage 11 Question*. Washington, DC: Am. Geophys. Union

Duncan RA, Hargraves RB. 1990. $^{40}Ar/^{39}Ar$ geochronology of basement rocks from the Mascarene Plateau, the Chagos Bank, and the Maldives Ridge. In *Proceedings of the Ocean Drilling Program, Scientific Results*, Vol. 115, pp. 43–51. College Station, TX: Ocean Drill. Program

Ebren P. 1996. *Impact des variations rapides du niveau marin sur le développement des atolls au quaternaire: Mururoa (Polynésie française). Dynamique récifale et diagenèse des carbonates.* PhD Thesis, Aix-Marseille Univ., Aix-en-Provence and Marseille, Fr.

Emiliani C. 1955. Pleistocene temperatures. *J. Geol.* 63:538–78

Fürstenau J, Lindhorst S, Betzler C, Hübscher C. 2010. Submerged reef terraces of the Maldives (Indian Ocean). *Geo-Mar. Lett.* 30:511–15

Gillot PY, Cornette Y, Guille G. 1992. Age (K-Ar) et conditions d'edification du soubassement volcanique de l'atoll de Mururoa (Pacifique Sud). *C. R. Acad. Sci.* 314:393–99

Gischler E, Hudson JH, Pisera A. 2008. Late Quaternary reef growth and sea level in the Maldives (Indian Ocean). *Mar. Geol.* 250:104–13

Gischler E, Humblet M, Braga JC, Eisenhauer A. 2018. Last interglacial reef facies and late Quaternary subsidence in the Maldives, Indian Ocean. *Mar. Geol.* 406:34–41

Grant GR, Naish TR, Dunbar GB, Stocchi P, Kominz MA, et al. 2019. The amplitude and origin of sea-level variability during the Pliocene epoch. *Nature* 574:237–41

Grimsdale TF. 1952. *Cycloclypeus (foraminifera) in the Funafuti boring, and its geological significance*. Occas. Pap., Chall. Soc. Mar. Soc., Southampton Oceanogr. Cent., Southampton, UK

Guille G, Buigues DC, Gachon A, Ruzié G. 1993. Structure et géologie de l'atoll de Mururoa. In *Atlas de la Polynésie Française*, ed. J-F Dupon, J Bonvallot, E Vigneron, plate 32. Paris: ORSTOM

Hoffmeister JE, Ladd HS. 1944. The antecedent-platform theory. *J. Geol.* 52:388–402

Hoffmeister JE, Ladd HS. 1945. Solution effects on elevated limestone terraces. *GSA Bull.* 56:809–18

Jorry SJ. 2014. PTOLEMEE cruise, RV L'Atalante. *Flotte Océanographique Française*. **https://doi.org/10.17600/14000900**

Jorry SJ, Camoin GF, Jouet G, Le Roy P, Vella C, et al. 2016. Modern sediments and Pleistocene reefs from isolated carbonate platforms (Iles Eparses, SW Indian Ocean): a preliminary study. *Acta Oecol.* 72:129–43

Jouet G, Deville E. 2015. PAMELA-MOZ4 cruise, RV Pourquoi pas? *Flotte Océanographique Française*. **https://doi.org/10.17600/15000700**

Kench PS. 1998. Physical controls on development of lagoon sand deposits and lagoon infilling in an Indian ocean atoll. *J. Coast. Res.* 14:1014–24

Kench PS. 2011. Tsunami. In *Encyclopedia of Modern Coral Reefs*, ed. D Hopley, pp. 359–63. Dordrecht, Neth.: Springer

Kench PS, Smithers SG, McLean RF, Nichol SL. 2009. Holocene reef growth in the Maldives: evidence of a mid-Holocene sea-level highstand in the central Indian Ocean. *Geology* 37:455–58

Kench PS, Thompson D, Ford MR, Ogawa H, McLean RF. 2015. Coral islands defy sea-level rise over the past century: records from a central Pacific atoll. *Geology* 43:515–18

Klostermann L, Gischler E. 2015. Holocene sedimentary evolution of a mid-ocean atoll lagoon, Maldives, Indian Ocean. *Int. J. Earth Sci.* 104:289–307

Koksal T. 2014. Evolution of North Malé Atoll rim during the last full glacial cycle (Malé Island, Republic of Maldives). MS Thesis, Rice Univ., Houston

Kuenen PH. 1933. *The Snellius Expedition in the Eastern Part of the Netherlands East-Indies, 1929–1930*. Leiden: E.J. Brill

Kuenen PH. 1954. Eniwetok drilling results. *Deep-Sea Res.* 1953:187–89

Ladd HS, Ingerson E, Townsend RC, Russell M, Stephenson HK. 1953. Drilling on Eniwetok Atoll, Marshall Islands. *AAPG Bull.* 37:2257–80

Lisiecki LE, Raymo ME. 2005. A Pliocene-Pleistocene stack of 57 globally distributed benthic $\delta^{18}O$ records. *Paleoceanography* 20:PA2007

Lüdmann T, Betzler C, Eberli GP, Reolid J, Reijmer JJG, et al. 2018. Carbonate delta drift: a new sediment drift type. *Mar. Geol.* 401:98–111

Lüdmann T, Kalvelage C, Betzler C, Fürstenau J, Hübscher C. 2013. The Maldives, a giant isolated carbonate platform dominated by bottom currents. *Mar. Pet. Geol.* 43:326–40

MacNeil FS. 1954. The shape of atolls; an inheritance from subaerial erosion forms. *Am. J. Sci.* 252:402–27

McManus JF, Oppo DW, Cullen JL. 1999. A 0.5-million-year record of millennial-scale climate variability in the North Atlantic. *Science* 283:971–75

McManus JF, Oppo DW, Cullen JL, Healey S. 2003. Marine Isotope Stage 11 (MIS 11): analog for Holocene and future climate? See Droxler et al. 2003, pp. 69–85

Miller KG, Browning JV, Schmelz WJ, Kopp RE, Moutain GS, et al. 2020. Cenozoic sea-level and cryospheric evolution from deep-sea geochemical and continental margin records. *Sci. Adv.* 6:eaaz1346

Miller KG, Kominz MA, Browning JV, Wright JD, Mountain GS, et al. 2005. The Phanerozoic record of global sea-level change. *Science* 310:1293–98

Miramontes E, Jorry SJ, Jouet G, Counts JW, Courgeon S, et al. 2019. Deep-water dunes on drowned isolated carbonate terraces (Mozambique Channel, south-west Indian Ocean). *Sedimentology* 66:1222–42

Montaggioni LF, Borgomano J, Fournier F, Granjeon D. 2015. Quaternary atoll development: new insights from the two-dimensional stratigraphic forward modelling of Mururoa Island (Central Pacific Ocean). *Sedimentology* 62:466–500

Naseer A. 2003. *The integrated growth response of coral reefs to environmental forcing: morphometric analysis of coral reefs of the Maldives*. PhD Thesis, Dalhousie Univ., Halifax, Can.

Nicora A, Premoli Silva I. 1990. Paleogene shallow-water larger foraminifers from Holes 714A and 715A, Leg 115, Indian Ocean. In *Proceedings of the Ocean Drilling Program, Scientific Results*, Vol. 115, ed. pp. 381–93. College Station, TX: Ocean Drill. Program

Ohde S, Greaves M, Masuzawa T, Buckley HA, Van Woesik R, et al. 2002. The chronology of Funafuti Atoll: revisiting an old friend. *Proc. R. Soc. A* 458:2289–306

Oppo DW, McManus JF, Cullen JL. 1998. Abrupt climate events 500,000 to 340,000 years ago: evidence from subpolar North Atlantic sediments. *Science* 279:1335–38

Owen A, Kruijsen J, Turner N, Wright K. 2011. *Marine energy in the Maldives: pre-feasibility report on Scottish support for Maldives marine energy implementation*. Rep., Cent. Underst. Sustain. Pract., Robert Gordon Univ. Aberdeen, UK

Perrin C. 1989. *Rôle des organismes dans l'édification et l'évolution de l'atoll de Mururoa (Polynésie française)*. PhD Thesis, Univ. Paris-Sud, Paris

Perry CT, Kench PS, Smithers SG, Yamano H, O'Leary M, Gulliver P. 2013. Time scales and modes of reef lagoon infilling in the Maldives and controls on the onset of reef island formation. *Geology* 41:1111–14

Purdy EG. 1974. Reef configurations: cause and effect. In *Reefs in Time and Space*, ed. LF Laporte, pp. 9–76. Tulsa, OK: Soc. Sediment. Geol.

Purdy EG, Bertram GT. 1993. *Carbonate Concepts from the Maldives, Indian Ocean*. Tulsa, OK: Am. Assoc. Pet. Geol.

Purdy EG, Gischler E. 2005. The transient nature of the empty bucket model of reef sedimentation. *Sediment. Geol.* 175:35–47

Purdy EG, Winterer EL. 2001. Origin of atoll lagoons. *GSA Bull.* 113:837–54

Purdy EG, Winterer EL. 2006. Contradicting barrier reef relationships for Darwin's evolution of reef types. *Int. J. Earth Sci.* 95:143–67

Raymo ME, Mitrovica JX. 2012. Collapse of polar ice sheets during the stage 11 interglacial. *Nature* 483:453–56

Rovere A, Khanna P, Bianchi CN, Droxler AW, Morri C, Naar DF. 2018. Submerged reef terraces in the Maldivian Archipelago (Indian Ocean). *Geomorphology* 317:218–32

Schlager W, Purkis SJ. 2013. Bucket structure in carbonate accumulations of the Maldive, Chagos and Laccadive archipelagos. *Int. J. Earth Sci.* 102:2225–38

Shackleton NJ. 1987. Oxygen isotopes, ice volume and sea level. *Quat. Sci. Rev.* 6:183–90

Shackleton NJ, Berger A, Peltier WR. 1990. An alternative astronomical calibration of the lower Pleistocene timescale based on ODP Site 677. *Earth Environ. Sci. Trans. R. Soc. Edinb.* 81:251–61

Shackleton NJ, Opdyke ND. 1973. Oxygen isotope and palaeomagnetic stratigraphy of equatorial Pacific core V28-238: oxygen isotope temperatures and ice volumes on a 10^5 year and 10^6 year scale. *Quat. Res.* 3:39–55

Smith WHF, Sandwell DT. 1997. Global sea floor topography from satellite altimetry and ship depth soundings. *Science* 277:1956–62

Spratt RM, Lisiecki LE. 2016. A Late Pleistocene sea level stack. *Clim. Past* 12:1079–92

Swart PK, Blättler CL, Nakakuni M, Mackenzie GJ, Betzler C, et al. 2019. Cyclic anoxia and organic rich carbonate sediments within a drowned carbonate platform linked to Antarctic ice volume changes: Late Oligocene-Early Miocene Maldives. *Earth Planet. Sci. Lett.* 521:1–13

Trichet J, Repellin P, Oustrière P. 1984. Stratigraphy and subsidence of the Mururoa atoll (French Polynesia). *Mar. Geol.* 56:241–57

UNEP-WCMC (UN Environ. Programme World Conserv. Monit. Cent.), WorldFish Cent., WRI (World Resour. Inst.), TNC (The Nat. Conserv.). 2018. *Global distribution of warm-water coral reefs, compiled from multiple sources including the Millennium Coral Reef Mapping Project*. Data Set, Version 4.0, UNEP-WCMC, Cambridge, UK. **http://data.unep-wcmc.org/datasets/1**

Wikipedia. 2020. Atoll. *Wikipedia*. **https://en.wikipedia.org/wiki/Atoll**

Yokoyama Y, Esat TM, Thompson WG, Thomas AL, Webster JM, et al. 2018. Rapid glaciation and a two-step sea level plunge into the Last Glacial Maximum. *Nature* 559:603–7